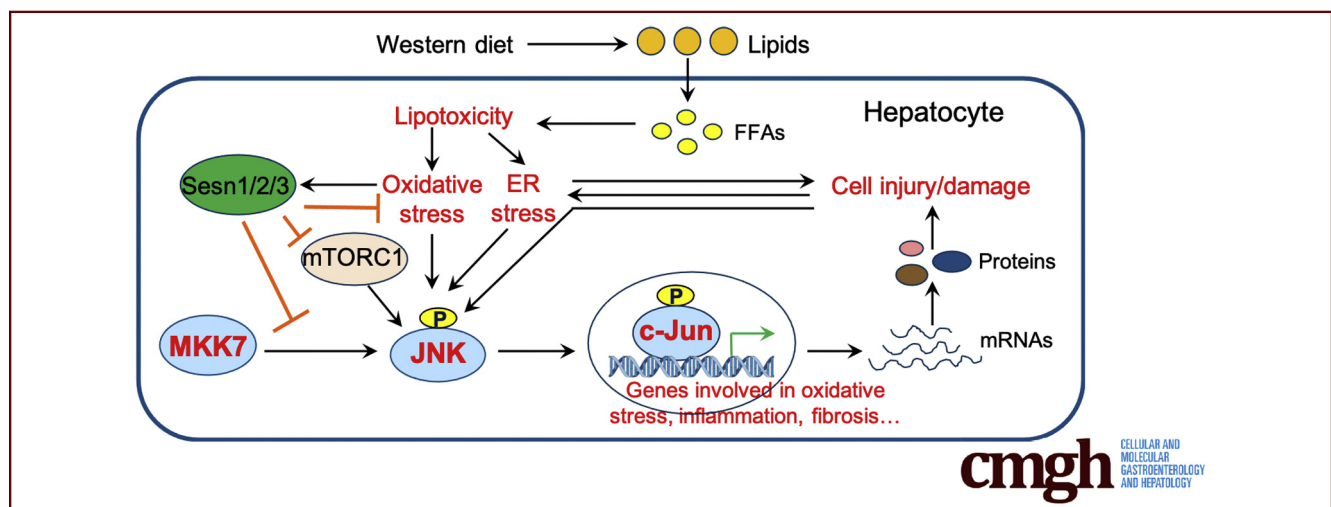


## ORIGINAL RESEARCH

## Sestrin Proteins Protect Against Lipotoxicity-Induced Oxidative Stress in the Liver via Suppression of C-Jun N-Terminal Kinases

Zhigang Fang,<sup>1,2,3,a</sup> Hyeong-Geug Kim,<sup>1,a</sup> Menghao Huang,<sup>1</sup> Kushan Chowdhury,<sup>1</sup> Ming O. Li,<sup>4</sup> Suthat Liangpunsakul,<sup>1,5,6</sup> and X. Charlie Dong<sup>1</sup><sup>1</sup>Department of Biochemistry and Molecular Biology, Indiana University School of Medicine, Indianapolis, Indiana;<sup>2</sup>Department of General Surgery, Guangzhou Digestive Disease Center, Guangzhou First People's Hospital, School of Medicine, South China University of Technology, Guangzhou, China; <sup>3</sup>The First Affiliated Hospital of Guangzhou University of Chinese Medicine, Guangzhou, China; <sup>4</sup>Immunology Program, Memorial Sloan Kettering Cancer Center, New York, New York; <sup>5</sup>Department of Medicine, Division of Gastroenterology and Hepatology, Indiana University School of Medicine, Indianapolis, Indiana; and <sup>6</sup>Roudebush Veterans Administration Medical Center, Indianapolis, Indiana

## SUMMARY

This work has identified a key role of Sesn1/2/3 proteins in the regulation of lipotoxicity-induced oxidative stress in the liver. Mechanistically, Sesn1/2/3 interact and inhibit JNK. Both in vitro and in vivo data demonstrate a strong liver-protective function of sestrins against lipotoxicity.

**BACKGROUND & AIMS:** Sestrin 1/2/3 (Sesn1/2/3) belong to a small family of proteins that have been implicated in the regulation of metabolic homeostasis and oxidative stress. However, the underlying mechanisms remain incompletely understood. The aim of this work was to illustrate the collective function of Sesn1/2/3 in the protection against hepatic lipotoxicity.

**METHODS:** We used *Sesn1/2/3* triple knockout (TKO) mouse and cell models to characterize oxidative stress and signal transduction under lipotoxic conditions. Biochemical, histologic, and physiological approaches were applied to illustrate the related processes.

**RESULTS:** After feeding with a Western diet for 8 weeks, TKO mice developed remarkable metabolic associated fatty liver

disease that was manifested by exacerbated hepatic steatosis, inflammation, and fibrosis compared with wild-type counterparts. Moreover, TKO mice exhibited higher levels of hepatic lipotoxicity and oxidative stress. Our biochemical data revealed a critical signaling node from sestrins to c-Jun N-terminal kinases (JNKs) in that sestrins interact with JNKs and mitogen-activated protein kinase kinase 7 and suppress the JNK phosphorylation and activity. In doing so, sestrins markedly reduced palmitate-induced lipotoxicity and oxidative stress in both mouse and human hepatocytes.

**CONCLUSIONS:** The data from this study suggest that Sesn1/2/3 play an important role in the protection against lipotoxicity-associated oxidative stress and related pathology in the liver. (*Cell Mol Gastroenterol Hepatol* 2021;12:921-942; <https://doi.org/10.1016/j.jcmgh.2021.04.015>)

**Keywords:** Sestrin; Oxidative Stress; C-Jun N-Terminal Kinase; Mitogen-Activated Protein Kinase Kinase 7; Lipotoxicity; Fatty Liver Disease.

Sestrin proteins (Sesn1/2/3) play an important role in the regulation of oxidative stress, endoplasmic reticulum (ER) stress, and metabolic homeostasis.<sup>1-16</sup>

Protein structural analysis of human SESN2 reveals an alkylhydroperoxidase activity against hydrophobic cumene hydroperoxide but not hydrophilic hydrogen peroxide (H<sub>2</sub>O<sub>2</sub>).<sup>17</sup> In addition to the intrinsic catalytic activity, sestrins also function through protein-protein interactions. Sestrins can activate AMP-activated protein kinase (AMPK) through an interaction with its alpha subunits.<sup>2</sup> Sestrins also activate mechanistic target of rapamycin complex 2 (mTORC2) through a direct interaction with rapamycin-insensitive companion of mTOR and GATOR2, whereas they inhibit mTORC1 by regulating GATOR2.<sup>16,18–20</sup>

Sestrin genes are regulated differently by cellular stress. The *Sesn1* gene is activated by transformation related protein 53 in response to genotoxic stress (ultraviolet,  $\gamma$ -irradiation, and cytotoxic drugs).<sup>21</sup> The *Sesn2* gene is induced by multiple stress stimuli including genotoxin, high-fat diet, oxidative stress, ER stress, hypoxia, and others.<sup>1,2,9,11,14,22–29</sup> The *Sesn3* gene is up-regulated by the forkhead box O (FoxO)-mediated stress pathways but down-regulated by diet or aging.<sup>4,13,30,31</sup> Genetic deletion of all 3 sestrin genes rather than single or double leads to high mortality rates postnatally,<sup>32,33</sup> suggesting a significant functional redundancy. *Drosophila* has a single *Sesn* gene (*dSesn*). Chronic TOR activation induces *dSesn* gene expression through oxidative stress-triggered activation of c-Jun amino-terminal kinase (JNK) and FoxO.<sup>11</sup> Loss of *dSesn* leads to triglyceride accumulation, mitochondrial defects, muscle degeneration, and cardiac malfunction.<sup>11</sup> *Sesn1* single or *Sesn1/2/3* triple knockout (TKO) mice have impaired exercise capacity.<sup>33,34</sup> *Sesn2* deficiency exacerbates high-fat diet-induced insulin resistance, glucose intolerance, and hepatic steatosis in mice.<sup>12,14</sup> Hepatic *Sesn3* deficiency in mice leads to insulin resistance and glucose intolerance.<sup>16</sup> *Sesn3* systemic knockout (KO) mice develop severe nonalcoholic steatohepatitis (NASH) on a Western diet (WD).<sup>4</sup>

In addition to the oxidoreductase activity, sestrins also protect cells against oxidative stress through positive regulation of AMPK and nuclear factor erythroid 2-related like 2 (NRF2) and negative regulation of mTORC1.<sup>1,2,5,11,12,35</sup> AMPK has been shown to mediate the sestrin antioxidative stress induced by doxorubicin in cardiomyocytes or lipopolysaccharide in mouse heart or endothelial cells.<sup>5,6,36</sup> NRF2 is a master regulator of antioxidant response. After feeding with a high-carbohydrate fat-free diet, *Sesn1/2* recruit the p62-mediated autophagy degradation machinery to degrade the NRF2 inhibitor, Kelch-like ECH-associated protein 1 (Keap1).<sup>1</sup> However, it remains unclear how sestrins are involved in lipotoxicity and what the underlying mechanisms are. This study aimed to address these questions.

## Results


### Hepatic *Sesn1/2/3* Deficiency Exacerbates Diet-Induced Fatty Liver Disease

To assess the role of sestrins in human metabolic associated fatty liver disease, we queried *SESN1/2/3* gene expression in the public datasets from the Gene Expression Omnibus database, and we found that hepatic *SESN1* and *SESN3* gene expression was trending down in hepatic

steatosis patients, whereas liver *SESN2* gene expression was trending down in human NASH patients (Figure 1A–C). Next, we examined the dietary effect on the expression of *Sesn1/2/3* genes in the liver of wild-type (WT) mice treated with a control diet or WD for 8 weeks. Hepatic *Sesn1/2/3* protein levels were decreased by 30%, 83%, and 66%, respectively, in the WD livers compared with that in the control diet livers (Figure 1D–G). To further investigate hepatic functions of the *Sesn1/2/3* genes, we generated hepatic *Sesn1/2/3* TKO mice by crossing *Sesn1* and *Sesn3* floxed mice with *Sesn2*<sup>-/-</sup> and Alb-Cre mice. Immunoblot analysis of *Sesn1/2/3* proteins in the liver and white adipose tissue confirmed that both *Sesn1* and *Sesn3* genes were specifically deleted in the liver on the background of the *Sesn2* gene global KO (Figure 2A and B). Next, we fed the animals with either the control diet or WD for 8 weeks. During the dietary treatment, WT, *Sesn2* knockout (*Sesn2*KO), and TKO mice had no significant difference in body weight on the same diet (Figure 2C). However, liver weight was significantly increased by 22% in the TKO mice as compared with that in the WT mice on WD, whereas white adipose tissue weight and liver or white adipose tissue to body weight ratios were not significantly different on either the control diet or WD (Figure 2D–G). WD induced a typical fatty liver phenotype manifested by a pale liver appearance and a significant increase in hepatic triglyceride and cholesterol levels in WT, *Sesn2*KO, and TKO mice as compared with the respective genotype on the control diet, with the lipid levels being highest in the TKO livers (Figure 2H–J, Figure 3A and B). Serum alanine aminotransferase levels were increased by 84% and 57% in the TKO mice as compared with those in the WT mice under the control diet and WD conditions, respectively (Figure 3C), suggesting that there was elevated liver injury in TKO mice. We performed immunohistochemical analysis of apoptosis in liver sections, and our data showed that TKO livers had increased cell death on the

<sup>a</sup>Authors share co-first authorship.

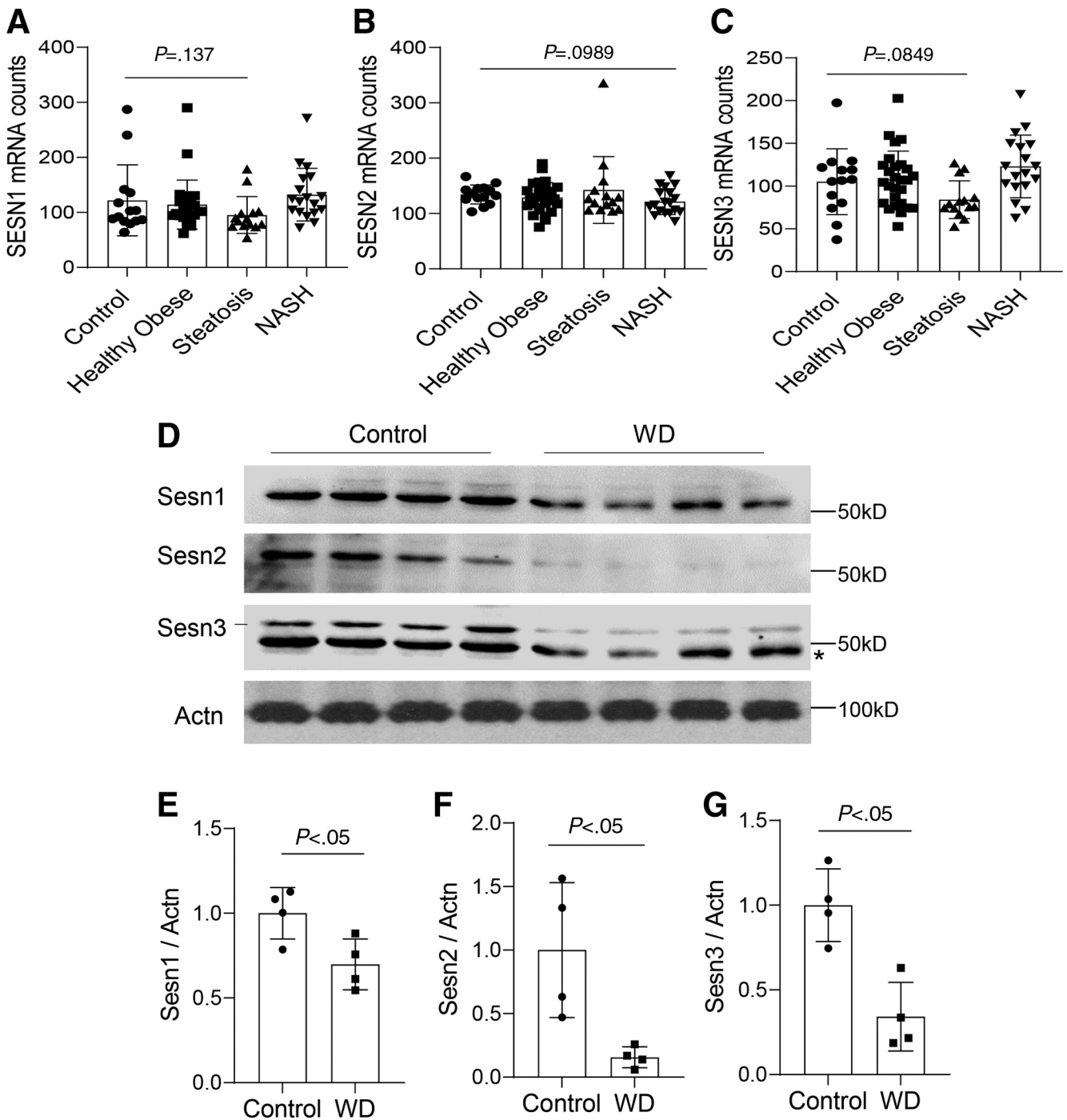
**Abbreviations used in this paper:** Acta2, smooth muscle actin alpha 2; AMPK, AMP-activated protein kinase; BSA, bovine serum albumin; Cat, catalase; Col1a1, collagen type 1 alpha 1; Dgat2, diacylglycerol O-acyltransferase 2; DHE, dihydroethidium; DMSO, dimethyl sulfoxide; ER, endoplasmic reticulum; Fasn, fatty acid synthase; FoxO, forkhead box O; Gpx3, glutathione peroxidase 3; GSH, glutathione; Gss, glutathione synthetase; 4-HNE, 4-hydroxynonenal; Il6, interleukin 6; JNK, c-Jun N-terminal kinase; KD, knockdown; Keap1, Kelch-like ECH-associated protein 1; KO, knockout; MDA, malondialdehyde; MKK, mitogen-activated protein kinase kinase; MPO, myeloperoxidase; mTORC, mechanistic target of rapamycin complex; Nox1, NADPH oxidase 1; NASH, nonalcoholic steatohepatitis; NF- $\kappa$ B, nuclear factor kappa B; NRF2, nuclear factor erythroid 2-related like 2; PA, palmitic acid; PCR, polymerase chain reaction; Pdgfrb, platelet-derived growth factor receptor beta; PERK, protein kinase R-like endoplasmic reticulum kinase; Scd1, stearoyl-CoA desaturase 1; SD, standard deviation; *Sesn1/2/3*, sestrin1/2/3; Sod, superoxide dismutase; Srebp, sterol regulatory element-binding protein; Tgfb1, transforming growth factor beta 1; Tgfb1, transforming growth factor beta receptor 1; Timp1, tissue inhibitor of metalloproteinase 1; TKO, triple knockout; Tnf, tumor necrosis factor; WD, Western diet; WT, wild-type.

 Most current article

© 2021 The Authors. Published by Elsevier Inc. on behalf of the AGA Institute. This is an open access article under the CC BY-NC-ND license (<http://creativecommons.org/licenses/by-nc-nd/4.0/>).

2352-345X

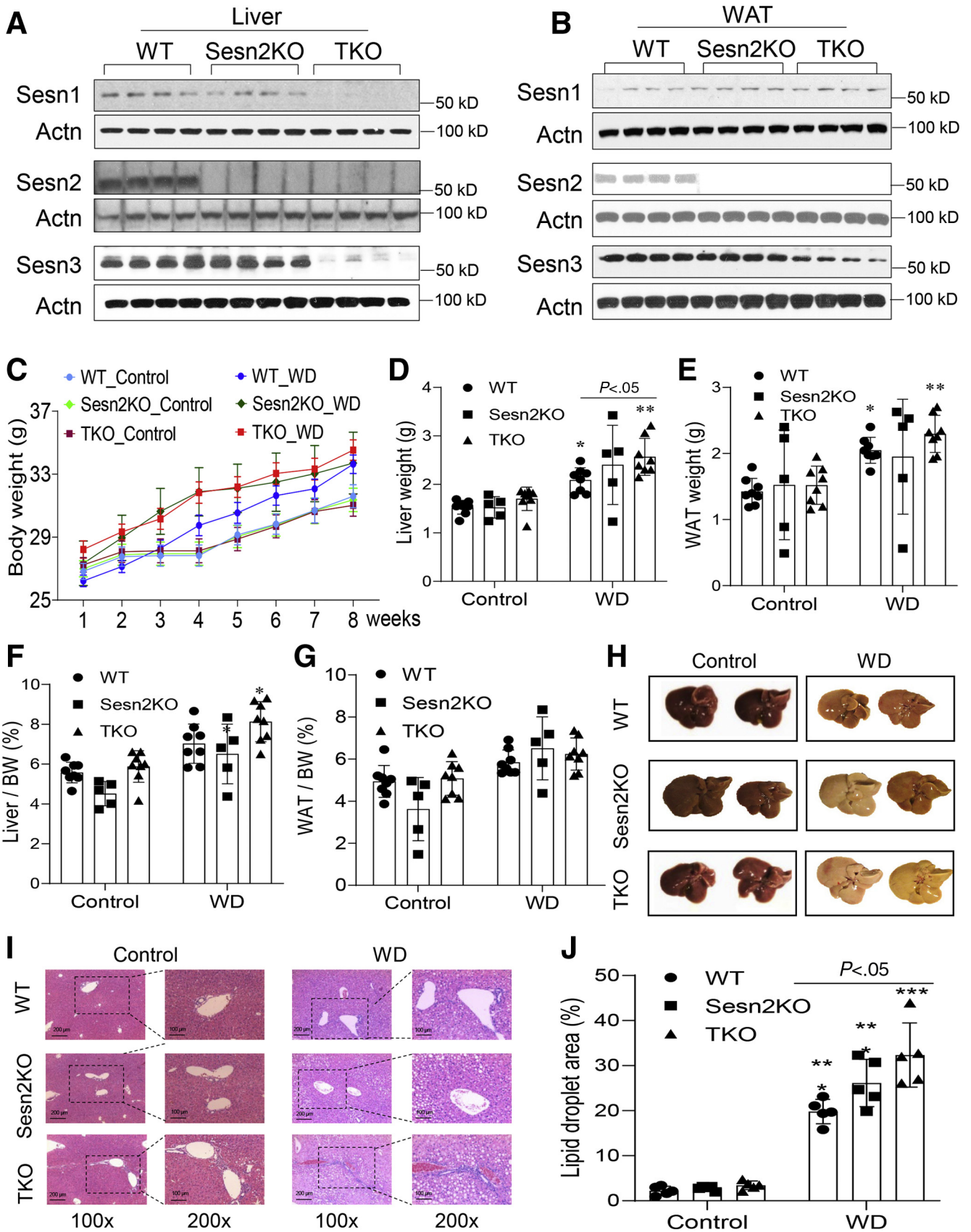
<https://doi.org/10.1016/j.jcmgh.2021.04.015>



**Figure 1. SESN1/2/3 gene expression in human and mouse livers under nonalcoholic fatty liver disease conditions.** (A–C) Human SESN1/2/3 gene expression in livers of obese, steatotic, and NASH patients. Human liver microarray data from Gene Expression Omnibus database (Accession: GSE48452) were downloaded and analyzed. Data are expressed as mean  $\pm$  standard deviation (SD) ( $n = 14$ – $27$ ). (D–G) Immunoblot and quantification analysis of Sesn1/2/3 in livers of WT mice treated with control diet or WD for 8 weeks. Data are expressed as mean  $\pm$  SD ( $n = 4$ ). \*Non-specific protein detected by the Sesn3 antibody.

control diet and even more so on WD compared with that in WT livers (Figure 3D and E). In addition, expression of lipogenic genes including sterol regulatory element-binding protein 1c (*Srebp1c*) and fatty acid synthase (*Fasn*) was significantly increased in the livers of TKO mice as

compared with WT mouse livers on the control diet (Figure 3F). *Srebp1a*, diacylglycerol O-acyltransferase 2 (*Dgat2*), and stearyl-CoA desaturase 1 (*Scd1*) genes were significantly up-regulated in the livers of TKO mice compared with the WT livers on WD (Figure 3G).





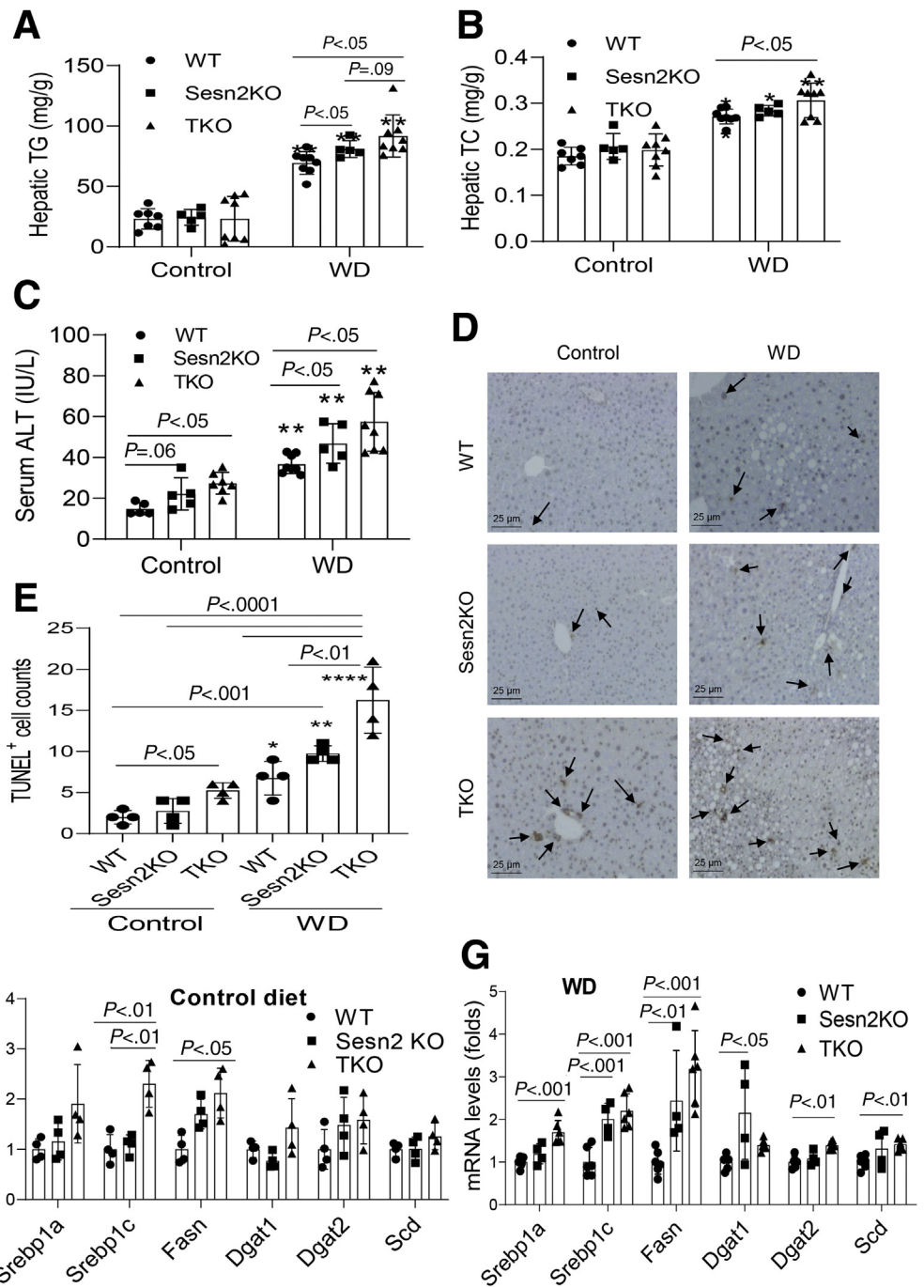


**Figure 3. *Sesn1/2/3* TKO mice are susceptible to WD-induced hepatic steatosis and liver injury.** (A) Hepatic triglyceride (TG) measurements in WT, *Sesn2KO*, and TKO mice fed with control diet or WD. (B) Hepatic total cholesterol (TC) measurements. (C) Serum alanine aminotransferase (ALT) levels. (D and E) Hepatic apoptosis analysis and quantification in liver sections using terminal deoxynucleotidyl transferase-mediated dUTP nick-end labeling (TUNEL) assays (original magnification, ×400). (F and G) Real-time PCR analysis of lipogenic genes in livers of control diet or WD treated mice. Data are expressed as mean ± SD (n = 4–8). \**P* < .05, \*\**P* < .01, or \*\*\*\**P* < .0001 for the respective genotype on WD vs control diet.

Next, we examined hepatic inflammation by immunostaining neutrophil and macrophage markers, myeloperoxidase (MPO) and F4/80, respectively. MPO<sup>+</sup> and F4/80<sup>+</sup> cell numbers were increased by 2.6- and 2.9- fold, respectively, in the TKO livers compared with those in the

WT livers (Figure 4A and B). Tumor necrosis factor (*Tnf*), a pro-inflammatory gene, was up-regulated, whereas interleukin 10 (*Il10*), an anti-inflammatory gene, was significantly down-regulated in the TKO livers compared with those in the WT livers on the control diet (Figure 4C). BCL2

**Figure 2. (See previous page). Genotyping and general characterization of *Sesn1/2/3* TKO mice.** (A and B) Western blot analysis of *Sesn1*, *Sesn2*, and *Sesn3* proteins in liver and white adipose tissue (WAT) of WT, *Sesn2KO*, and TKO mice. (C–G) Measurements of body weight, liver weight, WAT weight, liver to body weight ratio, and WAT to body weight ratio, respectively. (H) Liver images collected at end of the experiment. (I) H&E staining of liver sections. (J) Quantification of lipid droplet areas in liver sections of control diet or WD treated mice. Data are expressed as mean ± SD (n = 5–8). \**P* < .05, \*\**P* < .01, \*\*\**P* < .001 for WD vs control diet for the respective genotypes.

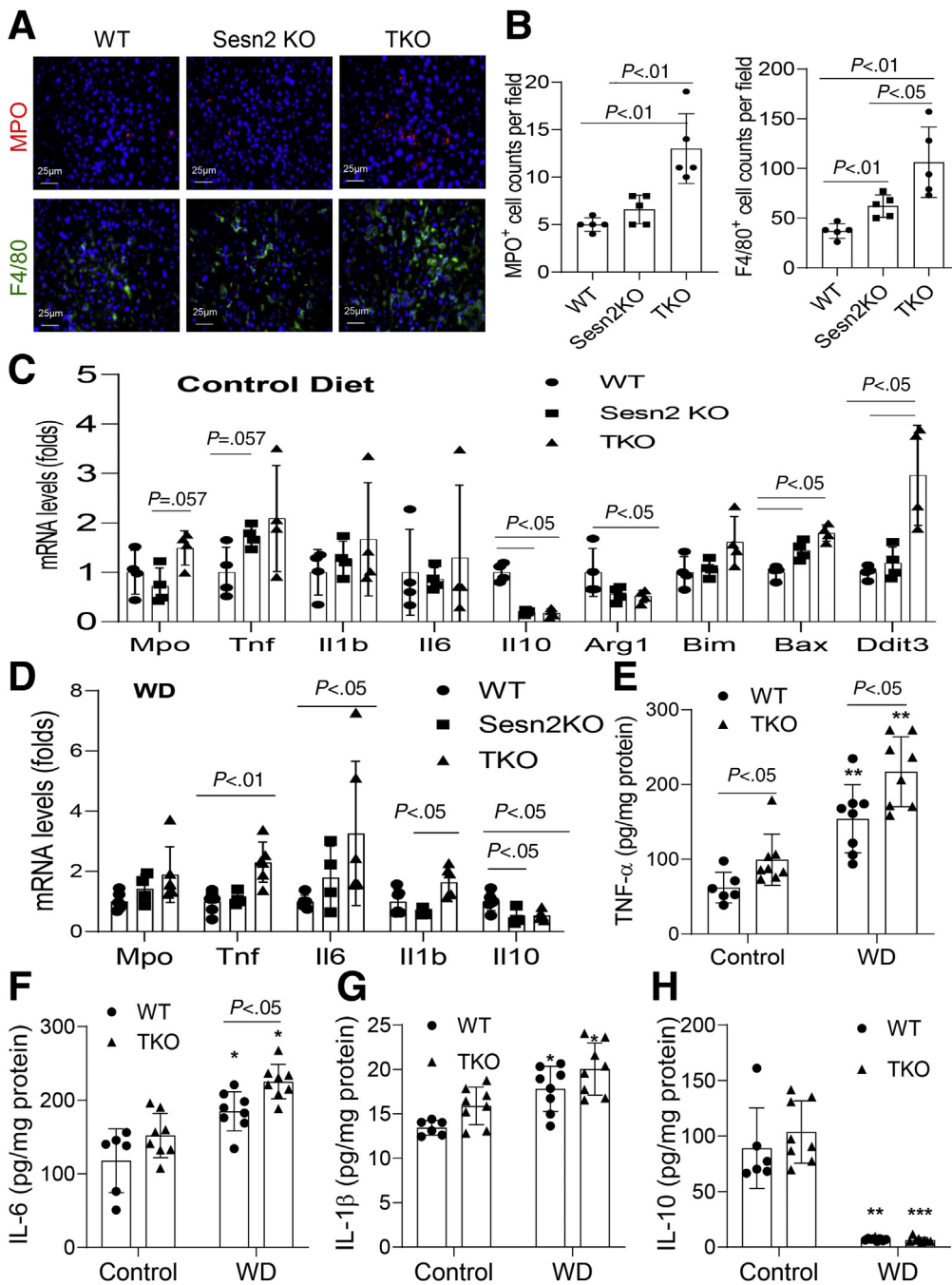
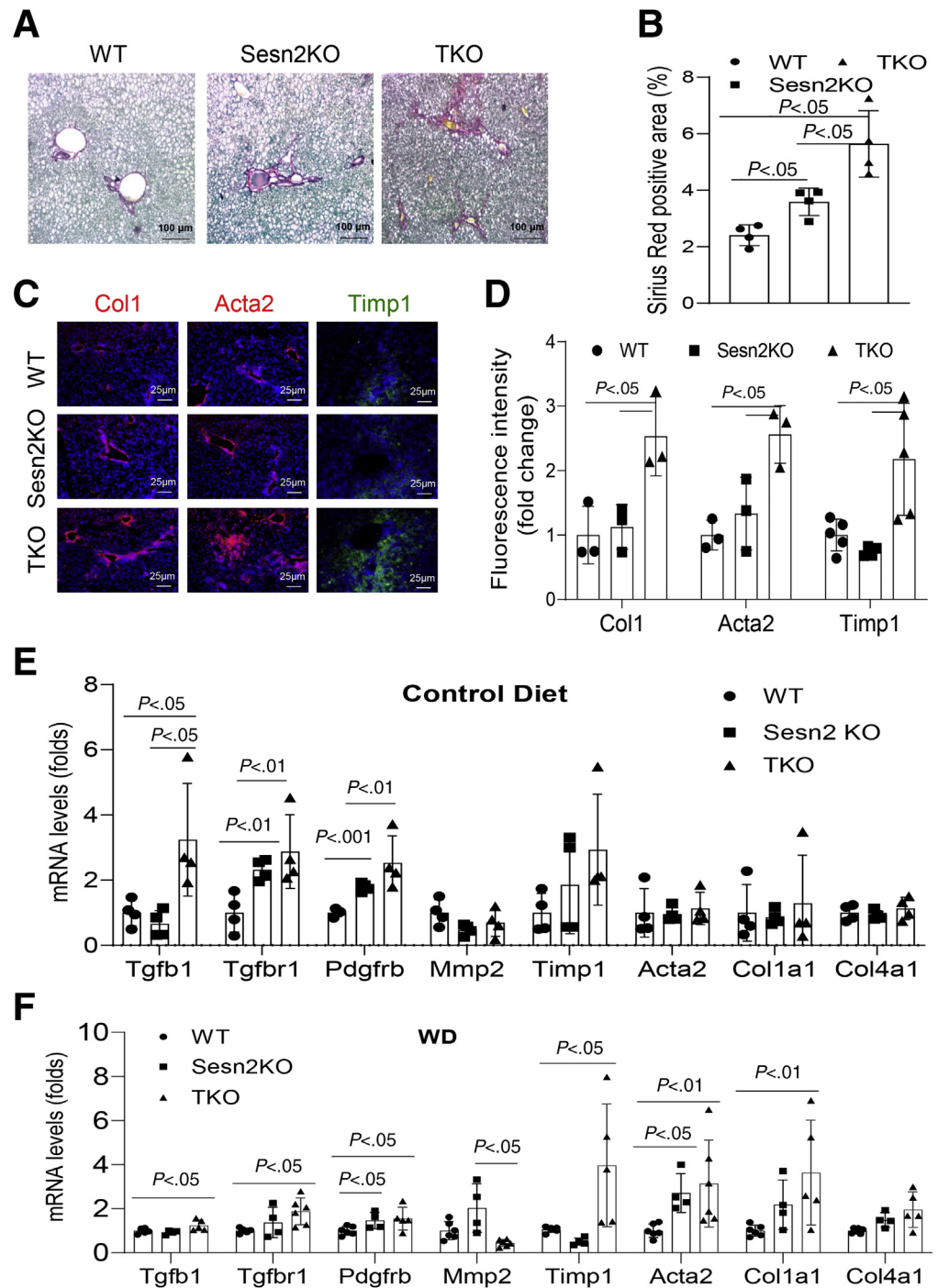


**Figure 4. *Sesn1/2/3* TKO mice manifest hepatic inflammation on WD.** (A) Immunofluorescence analysis of MPO and F4/80 in liver sections of WD-treated mice (original magnification,  $\times 100$ ). (B) Quantification of MPO- and F4/80-positive cells in (A). (C and D) Real-time PCR analysis of inflammation-related genes in livers of control diet or WD treated mice. (E–H) Hepatic cytokine levels were measured using enzyme-linked immunosorbent assay kits. Data are expressed as mean  $\pm$  SD ( $n = 4$ –5). \* $P < .05$ , \*\* $P < .01$ , and \*\*\* $P < .001$  for the respective genotype on WD vs control diet.

associated X apoptosis regulator (*Bax*) and DNA damage inducible transcript 3 (*Ddit3*, also called *Chop*), 2 proapoptosis genes, were significantly up-regulated in the livers of TKO mice compared with the WT livers on the control diet (Figure 4C). Similarly, the *Tnf*, *Il1b*, and *Il6* genes were up-regulated, whereas the *Il10* gene was down-regulated in the TKO livers compared with the WT livers on WD (Figure 4D). Hepatic TNF- $\alpha$  and IL6 protein levels were also elevated in the TKO mice compared with WT mice, whereas IL1 $\beta$  and IL10 levels were not significantly changed (Figure 4E–H). We also examined hepatic fibrosis by using multiple approaches in the WD treated mice. First,

liver sections were stained with a Sirius Red dye, and the data showed that hepatic fibrosis area was increased by 50% in the TKO mice compared with that in the WT mice (Figure 5A and B). Second, we performed immunofluorescent staining of 3 fibrosis-associated proteins, collagen type 1 (Col1), smooth muscle actin alpha 2 (Acta2), tissue inhibitor of metalloproteinase 1 (Timp1), and our data showed that all 3 fibrosis markers were significantly increased in the TKO livers compared with those in the WT livers (Figure 5C and D). Third, we analyzed expression of fibrosis-related genes including transforming growth factor beta 1 (*Tgfb1*), transforming growth factor beta



receptor 1 (*Tgfb1*), platelet-derived growth factor receptor beta (*Pdgfrb*), *Timp1*, *Acta2*, and *Col1a1* by real-time polymerase chain reaction (PCR), and our data showed that the *Tgfb1*, *Tgfb1*, and *Pdgfrb* genes were significantly induced in the TKO livers compared with those in the WT livers on both the control diet and WD, whereas the *Timp1*, *Acta2*, and *Col1a1* genes were up-regulated in the TKO livers compared with the WT livers only on WD (Figure 5E and F).

### *Sesn1/2/3* Gene Knockouts Exacerbate Diet-Induced Oxidative Stress

To investigate how *Sesn1/2/3* deficiency impacts WD-induced hepatic oxidative stress, we analyzed several markers of oxidative stress. Hepatic  $H_2O_2$  levels were increased by 63% and 88% in the TKO mice compared with those in the WT mice on the control diet and WD, respectively (Figure 6A). Hepatic nitric oxide levels were increased by 71% in the TKO mice compared with that in the WT mice



under the WD condition (Figure 6B). We also measured 2 lipid peroxidation markers, 4-hydroxynonenal (4-HNE) and malondialdehyde (MDA), by immunostaining and biochemical assays, respectively. Our data showed that 4-HNE and MDA levels were increased by 3-fold and 2-fold, respectively, in the TKO livers compared with the WT livers under the WD condition (Figure 6C and D). We also analyzed antioxidative responses to WD by measuring total glutathione (GSH) and superoxide dismutase (SOD) activity. Our data showed that GSH levels and SOD activities were decreased by 17% and 35%, respectively, in the TKO livers compared with the WT livers under the WD condition (Figure 6E and F). In addition, we analyzed expression of several oxidative stress related genes in the livers of WT and KO mice fed with the control diet or WD. On the control diet, glutathione synthetase (*Gss*) gene was significantly down-regulated, whereas glutathione peroxidase 3 (*Gpx3*) was significantly up-regulated in the TKO livers compared with the WT livers (Figure 6G). On WD, NADPH oxidase (*Nox1*), a pro-oxidative stress gene, was increased by 76%, whereas antioxidative stress genes such as *Gss*, *Gpx3*, *Sod1*, *Sod3*, and catalase (*Cat*) were significantly decreased in the TKO livers compared with the WT livers (Figure 6H).

To further examine whether the lipotoxicity-induced oxidative stress in the TKO liver primarily happens in hepatocytes, we treated primary hepatocytes from WT and TKO mice with either fatty acid-free bovine serum albumin (BSA) or BSA conjugated palmitic acids (PA) (200  $\mu\text{mol/L}$ ) for 18 hours and analyzed oxidative stress markers. Neutral lipid levels measured by BODIPY were increased by 74% in the TKO hepatocytes compared with the WT hepatocytes after the PA treatment (Figure 7A and B). CellROX, dihydroethidium (DHE), and 4-HNE positive signals were increased by 33%, 182%, and 31%, respectively, in the TKO hepatocytes compared with the WT hepatocytes treated with PA (Figure 7A and C-E). Immunoblot analysis also showed that 4-HNE modified proteins were increased by 66% in the PA-treated TKO hepatocytes compared with those in the WT hepatocytes (Figure 7F and G). *Sod2* was decreased in the TKO hepatocytes relative to the WT hepatocytes without the PA treatment, and PA further reduced *Sod2* in both WT and TKO hepatocytes (Figure 7F and H).

### *Sesn1/2/3* Inhibit Lipotoxicity-Triggered Oxidative Stress via Suppression of JNK

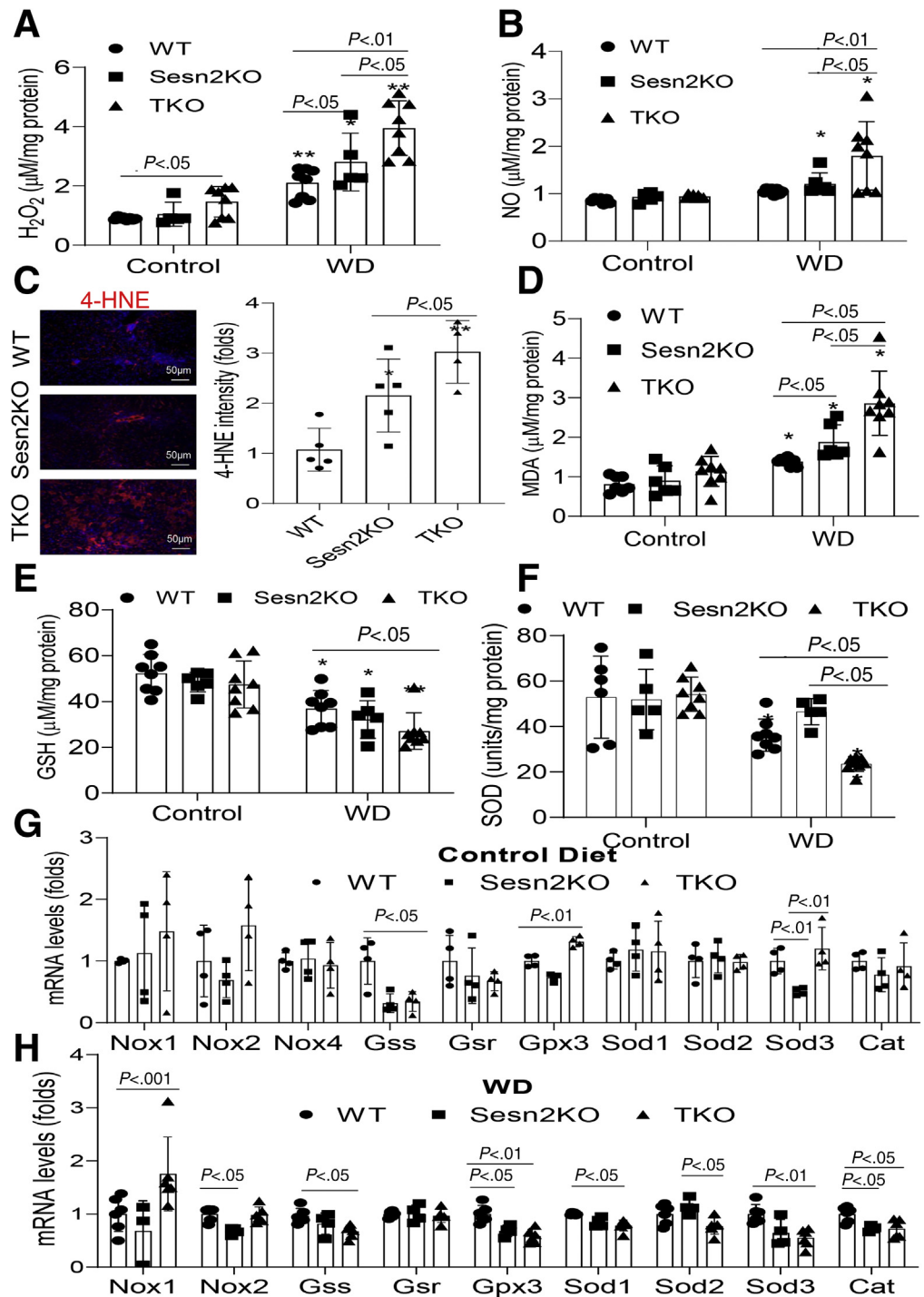
To investigate the mechanism underlying the oxidative stress in the TKO liver, we analyzed a stress-related kinase, JNK. Under the normal control diet condition, there was no significant difference in phosphorylated Jnk (p-Jnk Thr183/Tyr185) in the livers of WT, *Sesn2*KO, and TKO mice (Figure 8A and B). Next, we examined the effect of WD on Jnk phosphorylation. As expected, WD increased p-Jnk levels by 75% in the livers of WT mice as compared with the control diet (Figure 8C and D). In contrast, phosphorylated levels of mitogen-activated protein kinase kinase 7 (*Mkk7*, a kinase for Jnk), Jnk, c-Jun (a substrate of Jnk), nuclear factor kappa B (NF- $\kappa$ B), and p38 were increased by 2-, 8-, 15-, 2.3-, and 2.2-fold, respectively, in the TKO livers compared with

those in the WT livers under the WD condition (Figure 9A-F). We also performed immunostaining of p-Jnk in liver sections, and our data showed that hepatic p-Jnk levels were increased by 131% in the TKO mice compared with that in the WT mice (Figure 9G and H).

To corroborate the interaction between lipotoxicity and *Sesn1/2/3* genes, first, we isolated primary hepatocytes from WT and TKO mice and treated the cells with 200  $\mu\text{mol/L}$  PA for 18 hours. After the PA treatment, p-Mkk7, p-Jnk, p-c-Jun, and p-p38 levels were increased by 239%, 45%, 130%, and 156%, respectively, in the TKO hepatocytes compared with those in the WT hepatocytes (Figure 9I-M). Second, we generated *SESN1/2/3*-deficient HepG2 cells using the CRISPR/Cas9 technology. Gene knockdown (KD) was confirmed by immunoblotting (Figure 10A). We co-treated WT and *SESN1/2/3* KD cells with 200  $\mu\text{mol/L}$  PA and a JNK inhibitor SP600125 or control vehicle for 18 hours. Phosphorylated c-JUN positivity was increased by 85% in the KD cells compared with WT cells, and this difference was largely abolished by SP600125 (Figure 10B and C). The alteration of p-c-JUN by PA and SP600125 was also confirmed by immunoblot analysis (Figure 10D and E). Lipid peroxidation and intracellular  $\text{H}_2\text{O}_2$  levels were significantly elevated in the *SESN1/2/3* KD cells without the PA treatment and more dramatically increased with the PA treatment. Both oxidative stress indicators, 4-HNE and  $\text{H}_2\text{O}_2$ , were significantly decreased in the presence of the JNK inhibitor (Figure 10F-H).

To examine whether sestrins directly regulate Jnk, we performed co-immunoprecipitation analysis of *Sesn1/2/3* and Jnk2 in Huh7 cells after co-transfection of their plasmid DNAs. Our data showed an interaction between *Sesn1/2/3* and Jnk2 (Figure 11A). Moreover, we performed pull-down assays from Huh7 cells using Flag-tagged *Sesn1/2/3* after they were treated with 200  $\mu\text{mol/L}$  PA for 18 hours. *Sesn1/2/3*-Flag pulled down several kinases including JNK, MKK7, p38 MAPK, and AKT (a positive control) but not ERK (Figure 11B). We also observed that overexpression of *Sesn1/2/3* decreased p-JNK (Thr183/Tyr185), p-p38 (Thr180/Tyr182), and p-ERK (Thr202/Tyr204) levels (Figure 11B). To further explore how sestrins regulate JNK, we co-transfected Jnk2 and *Sesn3* in Huh7 cells and analyzed JNK and MKK7 interactions. We observed that *Sesn3* overexpression dramatically reduced the interaction between Jnk2 and endogenous MKK7 (Figure 11C). To verify whether the interaction between *Sesn3* and Jnk2 is required for the disruption of the JNK-MKK7 interaction, we generated N- and C-terminal truncated *Sesn3* constructs (amino acids 1-240 and 241-492, respectively) and found that C-terminal but not N-terminal *Sesn3* interacted with Jnk2. As predicted, only C-terminal *Sesn3* attenuated the interaction between Jnk2 and MKK7 (Figure 11D). Moreover, C-terminal *Sesn3* like full length suppressed phosphorylation of MKK7 and JNK after their overexpression in the Huh7 cells (Figure 11E). To further validate the protein-protein interactions in vivo, we performed 2 independent pull-down assays from mouse liver lysates using HA-tagged *Sesn3* transgenic mice or *Sesn1/2/3* antibodies. *Sesn3*-HA pulled





down Jnk, p-Jnk, Mkk7, and p38 Mapk but not Erk (Figure 12A). Similarly, Sesn1/2/3 antibodies also pulled down those kinases except Erk (Figure 12B). Taken together, these data suggest that sestrins interact with Mkk7, Jnk, and p38 Mapk in both hepatocytes and livers.

To further verify that sestrins suppress JNK and oxidative stress, we also used a gain-of-function approach by overexpressing individual sestrin genes in HepG2 cells and treating with 200  $\mu\text{mol/L}$  PA for 18 hours. Our data showed

that Sesn1/2/3 overexpression significantly decreased JNK and c-JUN phosphorylation and 4-HNE levels (Figure 13A-E). Because sestrins have also been implicated in the regulation of mTOR and ER stress, we analyzed the effect of Sesn1/2/3 deficiency and PA on these signaling pathways in control and *SESN1/2/3* KD HepG2 cells. Our data showed that PA exacerbated mTORC1 and protein kinase R-like endoplasmic reticulum kinase (PERK) activities as shown by elevated phosphorylation of S6 and eIF2 $\alpha$ ,

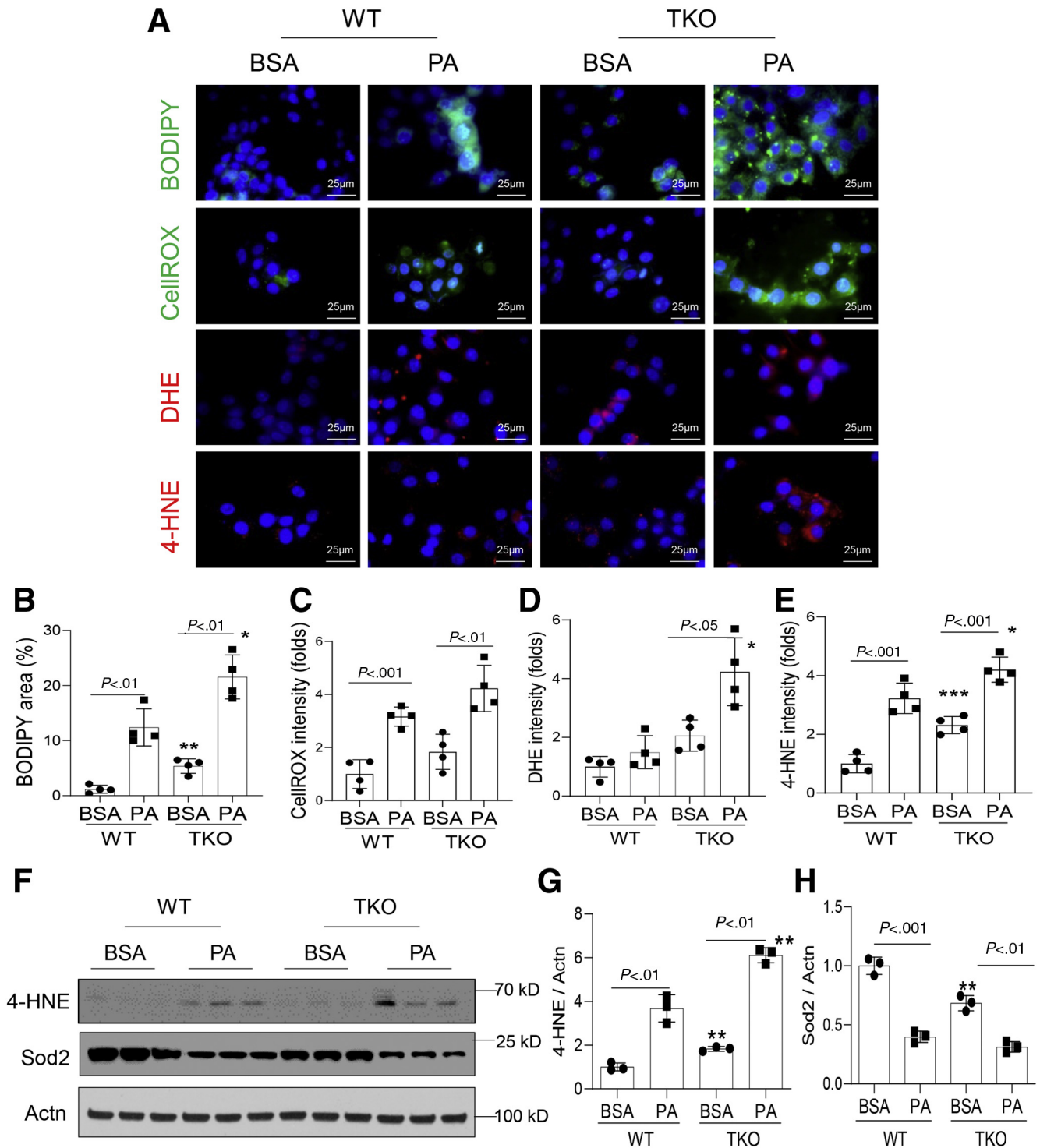


**Figure 7. *Sesn1/2/3* deficiency in hepatocytes exacerbates lipotoxicity-induced oxidative stress.** (A–E) Immunofluorescence imaging and quantification analysis of lipid droplets by BODIPY dye and oxidative stress by CellROX, DHE, and 4-HNE staining in WT and TKO mouse primary hepatocytes treated with control BSA or 200  $\mu$ mol/L PA conjugated in BSA for 18 hours, respectively (original magnification,  $\times 630$ ). (F–H) Immunoblotting and quantification analysis of 4-HNE and Sod2 in BSA or PA treated WT and TKO mouse primary hepatocytes. Data are expressed as mean  $\pm$  SD ( $n = 3$ –4). \* $P < .05$ , \*\* $P < .01$ , or \*\*\* $P < .001$  for TKO vs WT hepatocytes under the same treatments.

respectively (Figure 14A and B). To further examine a potential crosstalk between sestrins and mTORC1, PERK, and oxidative stress in the regulation of JNK, we treated control

and *SESN1/2/3* KD HepG2 cells with rapamycin (an mTORC1 inhibitor), GSK2656157 (a PERK inhibitor), and N-acetyl cysteine (an antioxidant) together with 200  $\mu$ mol/L

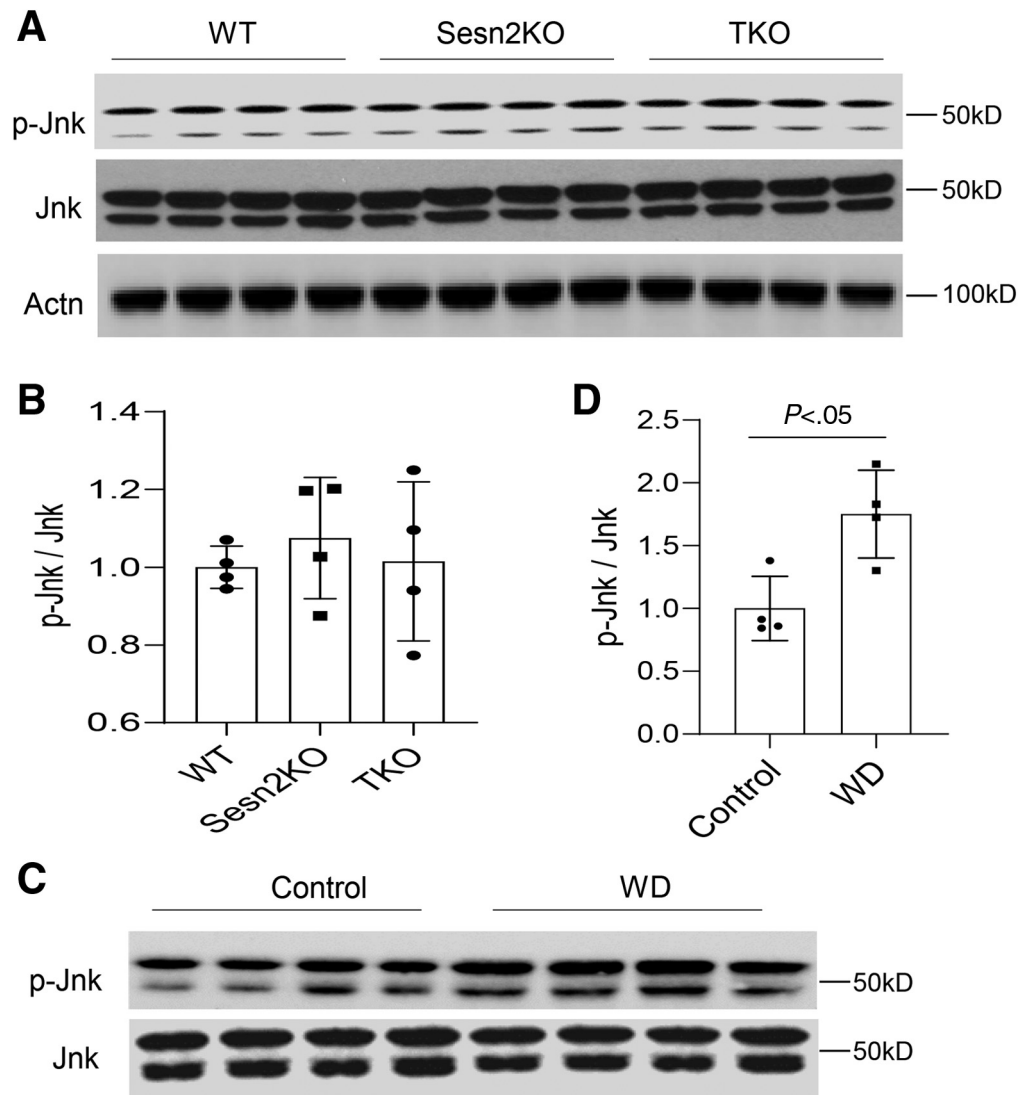


**Figure 8. Jnk phosphorylation levels are not elevated in TKO mouse livers on the control diet.** (A and B) Immunoblot and quantification analysis of p-Jnk (Thr183/Tyr185) in the livers of WT, Sesn2KO, and TKO mice fed with control diet. (C and D) Immunoblot and quantification analysis of p-Jnk (Thr183/Tyr185) in livers of WT mice fed with either control diet or WD. Data are expressed as mean  $\pm$  SD (n = 4).

PA. The data showed that inhibition of mTORC1 or PERK or attenuation of oxidative stress reduced the lipotoxicity-induced JNK activation (Figure 15A–J). These data suggest that under the lipotoxic conditions, JNK is subjected to regulation by multiple factors including sestrins, mTORC1, ER stress, and oxidative stress.

## Discussion

It has been widely reported that saturated fatty acids such as palmitates can induce oxidative stress and even cell death.<sup>37</sup> In this work, we demonstrate the protective effect of Sesn1/2/3 against hepatic lipotoxicity. Our results are consistent with several previous studies on the hepatoprotective role of sestrins through various mechanisms.<sup>1,4,7–9,12–14,16,38–41</sup> *Sesn2*<sup>-/-</sup> mice are susceptible to high-fat-induced hepatic steatosis and ER stress due to decreased AMPK and increased mTORC1 activities.<sup>12,14</sup> Sesn2 also protects high-carbohydrate fat-free diet-induced liver injury through p62-dependent

autophagic degradation of Keap1 and activation of NRF2.<sup>1</sup> We have recently reported a key role of Sesn3 in the suppression of the TGF $\beta$ -SMAD3 pathway during NASH development.<sup>4</sup> In addition, Sesn3 deficiency significantly increases carcinogen-triggered hepatocellular carcinoma development through activation of the hedgehog signaling pathway.<sup>13</sup> Our data from the current study have shown that Sesn1/2/3 have redundant functions in the liver because TKO mice manifest worse fatty liver phenotype than Sesn2KO mice, especially in hepatic inflammation, fibrosis, and oxidative stress.

In this work, we have explored the mechanism for the Sesn1/2/3 functions in the control of hepatic lipotoxicity and have identified JNK as a key regulatory point. Our biochemical characterization has revealed a direct protein-protein interaction between Sesn1/2/3 and JNK2. Functional analysis suggests that the interactions inhibit the JNK phosphorylation and activity. Because JNK kinases both respond to and enhance oxidative stress,<sup>42</sup> attenuation of the JNK activity by sestrins can be very helpful to

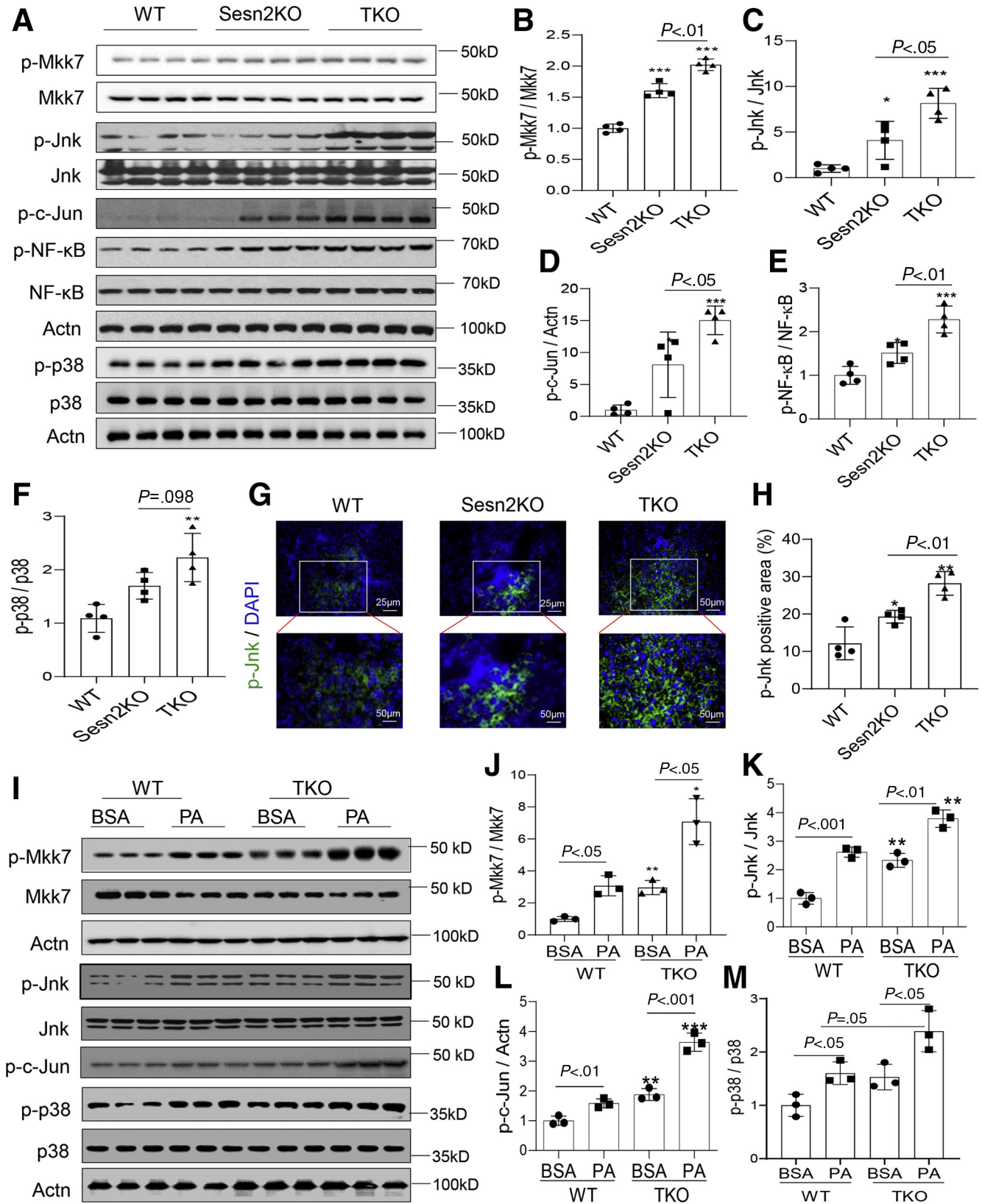
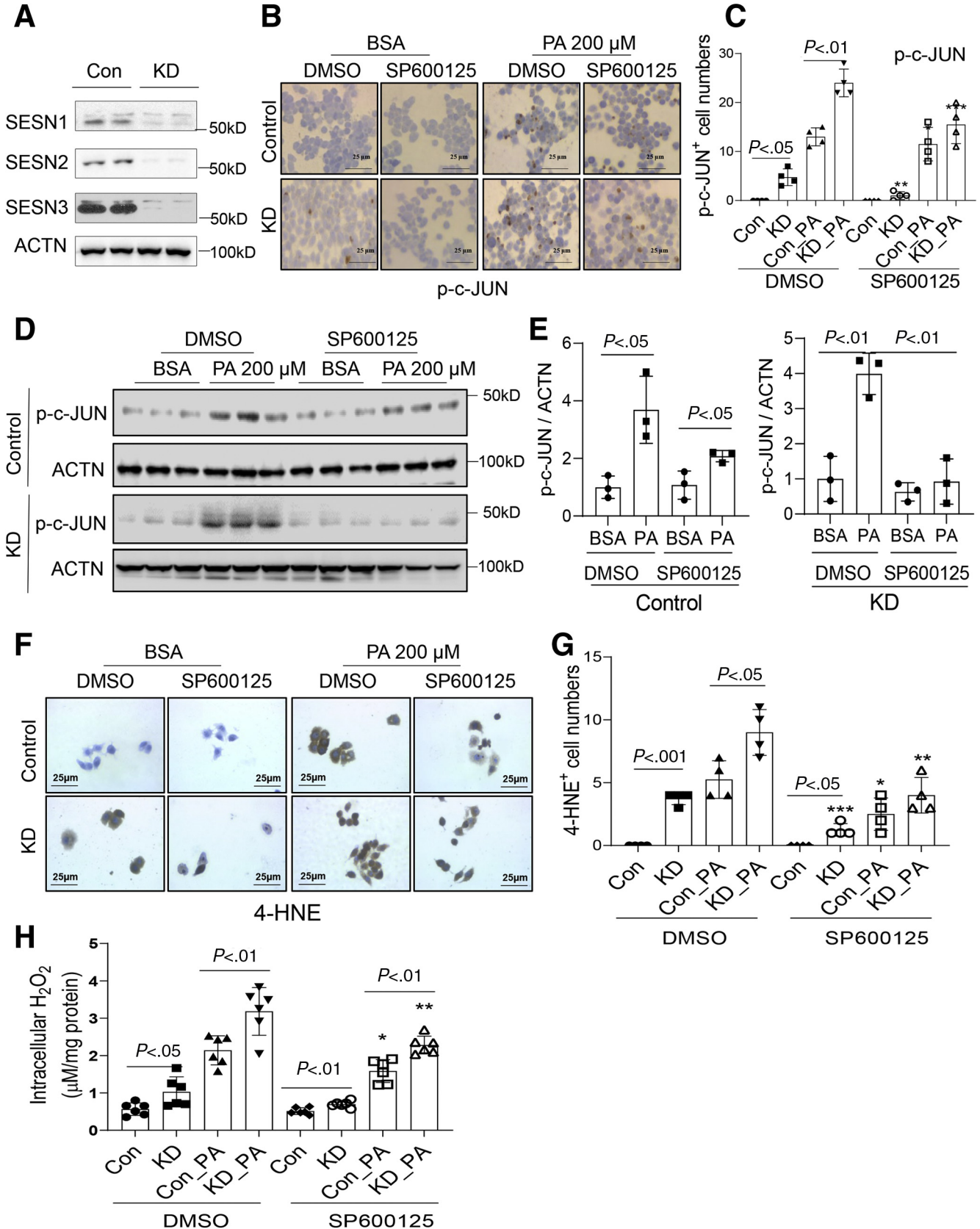


**Figure 9. Jnk activity is elevated in the Sesn1/2/3-deficient liver on WD.** (A–F) Immunoblot and quantification analysis of total and phosphorylated Mkk7, Jnk, c-Jun, NF-κB, and p38 in livers of WD treated mice. (G and H) Immunofluorescence and quantification analysis of phosphorylated Jnk in liver sections of WD treated mice (original magnification, ×200). (I–M) Immunoblot and quantification analysis of total and phosphorylated Mkk7, Jnk, c-Jun, and p38 in WT and TKO mouse primary hepatocytes treated with BSA or 200 μmol/L PA for 18 hours. Data are expressed as mean ± SD (n = 3–4). \* $P < .05$ , \*\* $P < .01$ , or \*\*\* $P < .001$  vs WT.



control oxidative stress within the cell tolerance range. Interestingly, sestrins have been shown to activate ERK, JNK, and p38 MAPK in the same protein complex in

senescent T lymphocytes.<sup>43</sup> Our data suggest that sestrins interact with JNK and p38 MAPK but not ERK1/2 in hepatocytes. The differential regulation of JNK among



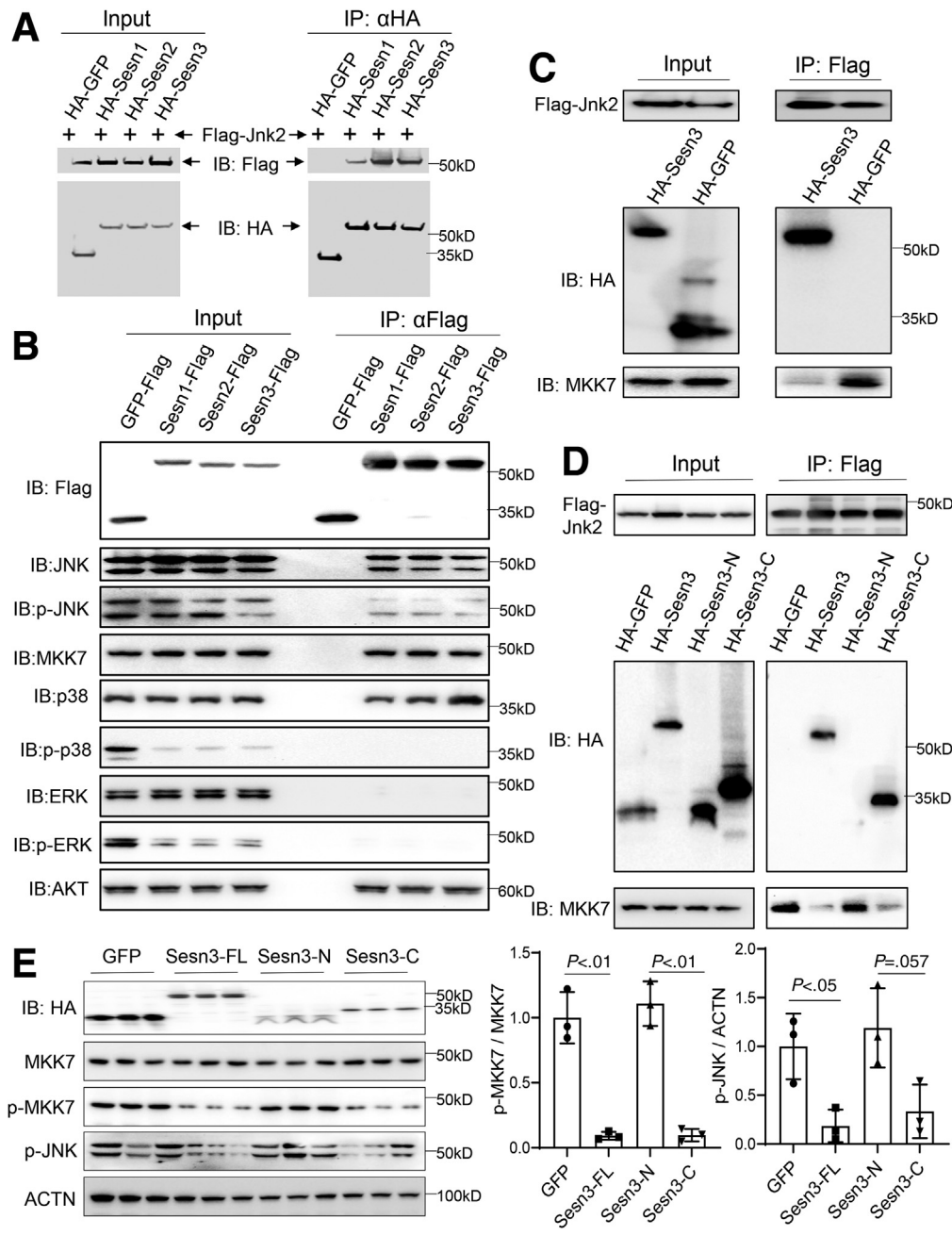


**Figure 11. Sestrins interact with Jnk in hepatocytes.** (A) Co-immunoprecipitation (IP) analysis of interactions between Sesn1/2/3 and Jnk2 in Huh7 cells after co-transfection of the indicated plasmids. IP reactions were performed with anti-HA monoclonal antibody beads. (B) Pull-down analysis of endogenous kinases by Flag-tagged Sesn1, Sesn2, and Sesn3 in Huh7 cells after treatment with 200  $\mu$ mol/L PA for 24 hours. (C) Co-IP analysis of interactions between Jnk2 and Sesn3 and MKK7 after transfection of Flag-Jnk2 and HA-Sesn3 in Huh7 cells for 48 hours. (D) Pull-down analysis of Jnk2 and MKK7 after transfection of Flag-Jnk2 and N-terminal or C-terminal truncated Sesn3 (Sesn3-N and Sesn3-C, respectively) plasmids in Huh7 cells for 48 hours. (E) Immunoblot analysis of MKK7 and JNK phosphorylation levels after transfection of either full-length (FL) or truncated Sesn3 plasmids in Huh7 cells for 48 hours. Data are expressed as mean  $\pm$  SD (n = 3). \* $P < .05$  and \*\* $P < .01$  vs green fluorescent protein (GFP).

different cell types requires further comparative studies. In addition, our data also suggest that sestrins interact with MKK7, which is an upstream kinase for JNK.<sup>44</sup> These data implicate that Sesn1/2/3 could suppress the JNK signaling pathway through inhibition of JNK

phosphorylation by MKK7. At this time, the detailed mechanism remains to be determined. We surmise that binding of Sesn1/2/3 to JNK could directly interfere with the JNK Thr183 phosphorylation by MKK7. In addition, Sesn1/2/3 may indirectly regulate the JNK activity

**Figure 10. (See previous page). SESN1/2/3 gene KD in human hepatocytes increases lipotoxicity and JNK activity.** (A) Confirmation of SESN1/2/3 triple KDs in HepG2 cells by immunoblotting. (B–E) Analysis of phosphorylated c-JUN by immunocytochemistry (original magnification,  $\times 400$ ) and immunoblotting in HepG2 cells treated with control DMSO or a JNK inhibitor SP600125 (10  $\mu$ mol/L) for 6 hours, followed by incubation with BSA or 200  $\mu$ mol/L PA for 18 hours. (F–H) Immunocytochemical and biochemical analysis of 4-HNE and H<sub>2</sub>O<sub>2</sub> in control or SESN1/2/3 KD HepG2 cells after treatment with DMSO or SP600125 for 6 hours, followed by incubation with BSA or 200  $\mu$ mol/L PA for 18 hours. Data are expressed as mean  $\pm$  SD (n = 3–6). \* $P < .05$ , \*\* $P < .01$ , or \*\*\* $P < .001$  vs DMSO.

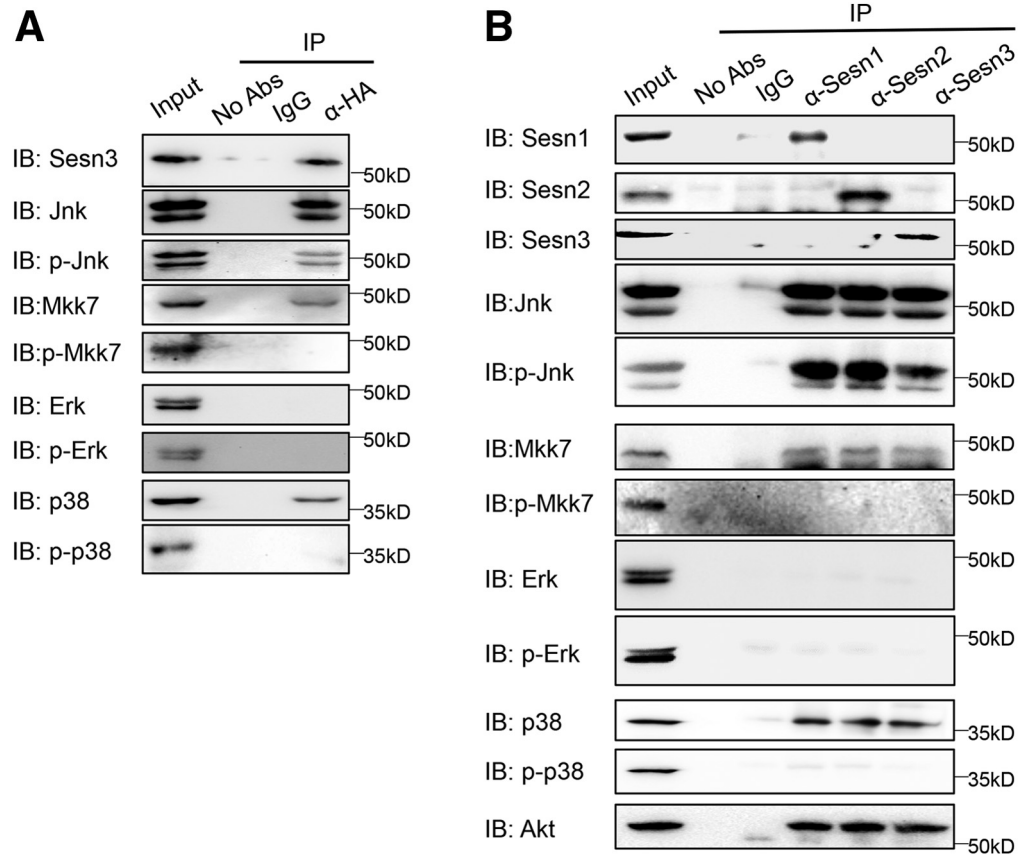


**Figure 12. Sestrins interact with Jnk in mouse livers.** (A) Sesn3 pulled down Mkk7, Jnk, and p38 MAPK from liver extracts of WD treated Sesn3 transgenic mice (Sesn3 transgene with HA tag) using anti-HA antibody beads. (B) Immunoprecipitation analysis of sestrin-interacting proteins in WD treated WT livers using Sesn1/2/3 antibodies.

through the mTOR signaling, ER stress, or oxidative stress because our data showed that inhibition of mTORC1 or PERK or attenuation of oxidative stress reduces the JNK phosphorylation even in the *Sesn1/2/3* KD cells.

In summary, our data strongly suggest a protective effect of Sesn1/2/3 against lipotoxicity and oxidative stress in the liver. Through the suppression of the JNK activity, sestrins break the vicious cycle of reactive oxygen species production and lipid peroxidation and their pathogenic sequelae. Considering this and other salutary functions of sestrins, we believe that positively modulating sestrin activity can be an attractive strategy for NASH therapeutic development.

## Materials and Methods

### Animal procedures

**Animals.** All animal care and experimental procedures performed in this work were approved by the Institutional Animal Care and Use Committee of Indiana University School of Medicine in accordance with National Institutes of Health guidelines for the care and use of laboratory animals. *Sesn1*, *Sesn2*, and *Sesn3* KO mice were generated as previously described.<sup>32</sup> *Sesn1* and *Sesn3* liver-specific KOs on the background of *Sesn2* systemic KO mice (TKO) were generated by crossing *Sesn1/3* floxed mice with an Alb-Cre strain and *Sesn2*<sup>-/-</sup> mice. *Sesn3* transgenic mice were generated as previously described.<sup>4</sup> Mice were

housed in an animal facility with controlled temperature (22° ± 2°C), humidity (60% ± 5%), and a regular 12:12 light/dark cycle. Animals were fed a control diet that is composed of 18 kcal% fat, 58 kcal% carbohydrate, and 24 kcal% protein or a WD (Research Diets Inc, New Brunswick, NJ) that contains 40 kcal% fat, 20 kcal% fructose, and 1% cholesterol for 8 weeks. Body weight was measured weekly. At the end of the experiments, mice were euthanized under anesthesia for blood and tissue collection.

**Genotyping.** *Sesn1/2/3* KO mice were genotyped by PCR analysis and confirmed by immunoblotting. Genotyping PCR primers are described in Table 1. The following antibodies were used for immunoblotting: rabbit anti-Sesn1 polyclonal antibody (PA-526881; Invitrogen, Waltham, MA), rabbit anti-Sesn2 polyclonal antibody (PA-572834; Invitrogen), and rabbit anti-Sesn3 polyclonal antibody (PIPA522220; Thermo Fisher Scientific, Waltham, MA).

### Biochemical Analysis

Serum alanine aminotransferase was measured using a commercial kit according to the manufacturer's manual (Thermo Fisher Scientific). Hepatic total cholesterol and triglycerides were analyzed using commercial assay kits (Wako USA, Richmond, VA). Tissue and cellular hydrogen peroxide (H<sub>2</sub>O<sub>2</sub>) and nitric oxide were measured using commercial assay kits (Invitrogen, and BioVision, Milpitas, CA). Lipid peroxidation was determined using an assay kit



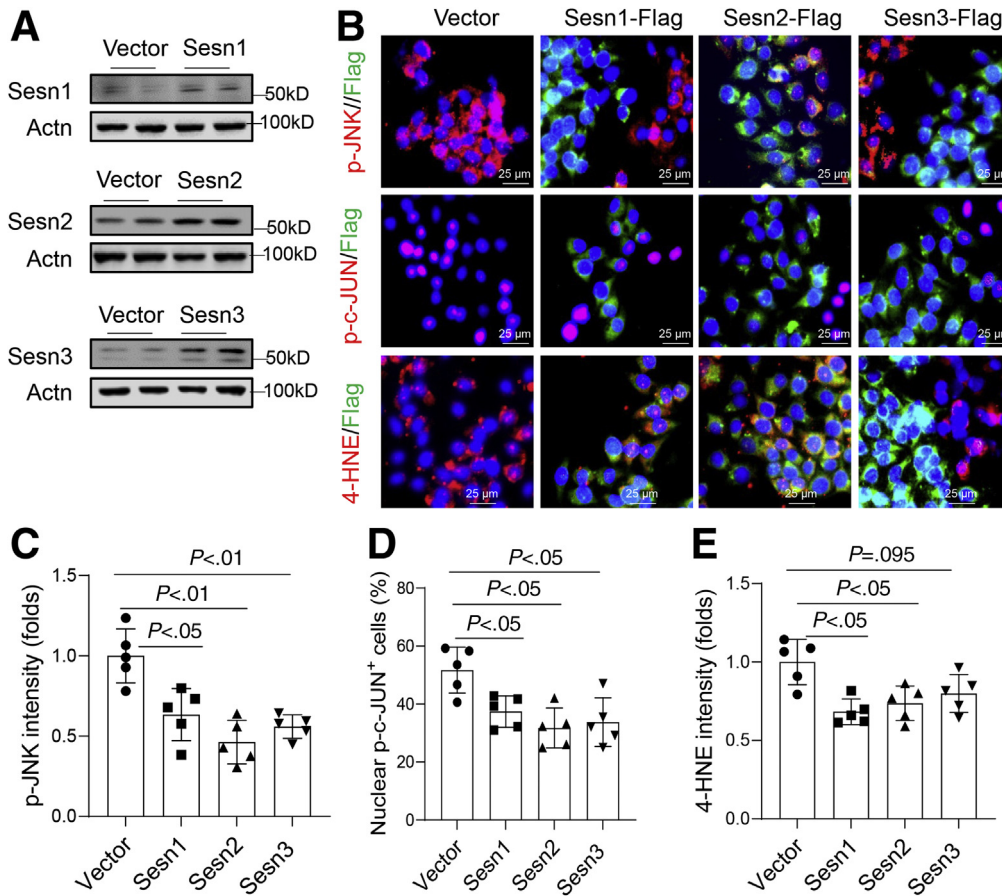


**Figure 13. Sesn1/2/3 overexpression suppresses JNK and lipotoxicity in human hepatocytes.** (A) Confirmation of Sesn1/2/3 overexpression in HepG2 cells by immunoblotting. (B–E) Immunofluorescence imaging and quantification of p-JNK, p-c-JUN, and 4-HNE in the HepG2 cells overexpressed with vector, Sesn1, Sesn2, or Sesn3 and treated with 200  $\mu\text{mol/L}$  PA for 18 hours. Data are expressed as mean  $\pm$  SD (n = 5).

for MDA (BioAssay Systems, Hayward, CA). GSH and SOD were analyzed using assay kits from Sigma-Aldrich (St Louis, MO). Tissue cytokines were measured using commercial enzyme-linked immunosorbent assay kits (mouse TNF- $\alpha$  and mouse IL6 from BD Biosciences, San Jose, CA; mouse IL1 $\beta$  and mouse IL10 from R&D Systems, Minneapolis, MN) following the manufacturer’s instructions.

**mRNA Analysis**

Total RNAs were isolated from cells and tissues using TRI reagent from Sigma-Aldrich. cDNA was synthesized using a reverse transcription kit (Invitrogen). Real-time PCR analysis was performed using a SYBR Green qPCR kit (Invitrogen). Primer sequences are described in Table 1.

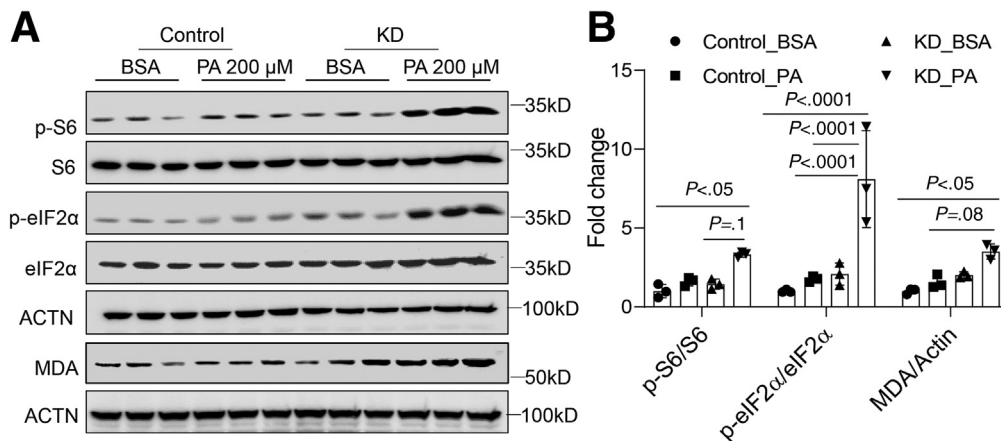
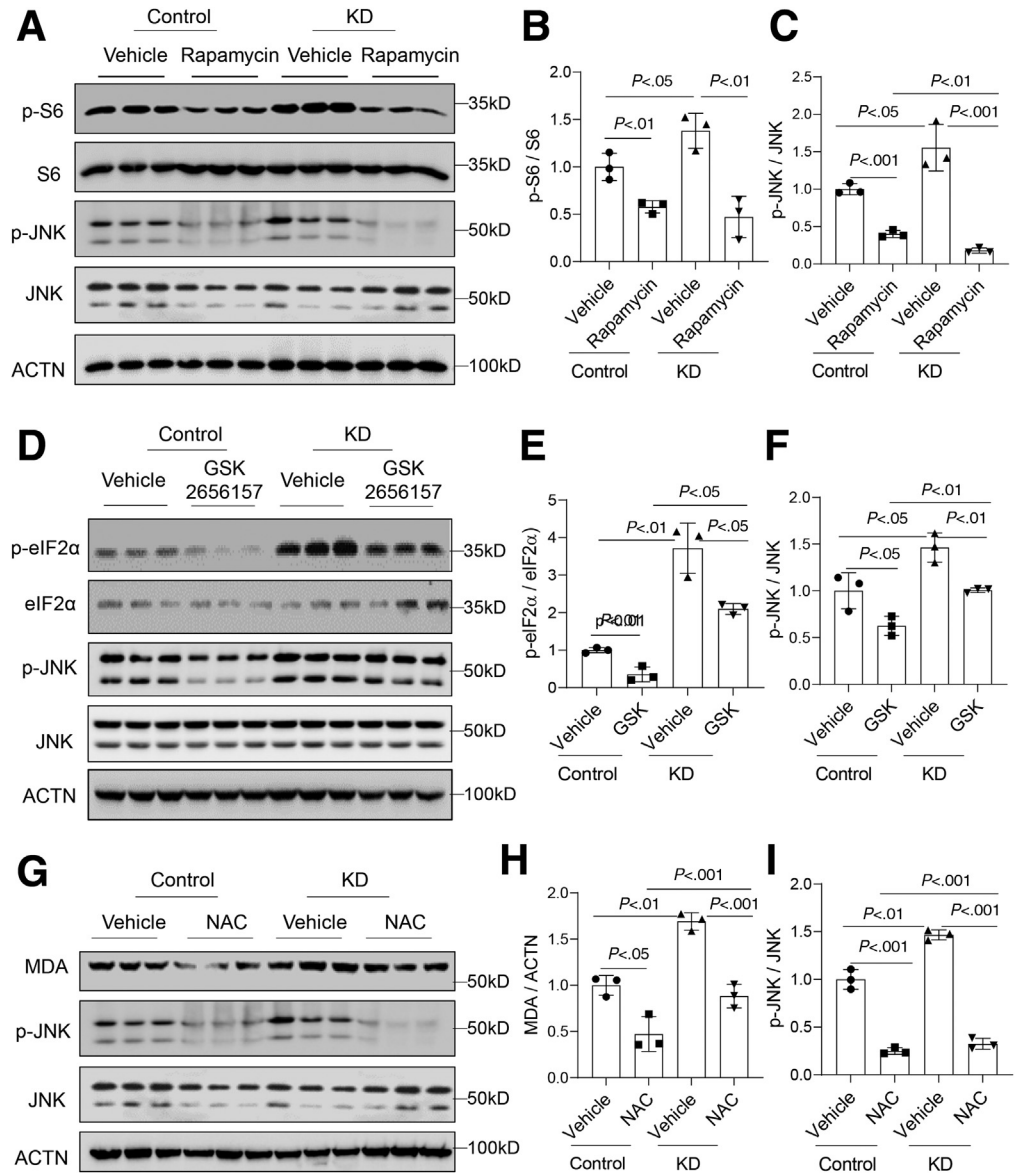


**Figure 14. Sesn1/2/3 deficiency exacerbates palmitate-induced ER stress and lipid peroxidation.** (A and B) Immunoblotting and quantification analysis of mTORC1 signaling (p-S6 as a readout), ER stress (p-eIF2 $\alpha$  as a readout), and lipid peroxidation (MDA-modified proteins as a readout) in control and SESN1/2/3 KD HepG2 cells treated with control BSA or 200  $\mu\text{mol/L}$  PA for 24 hours. Data are expressed as mean  $\pm$  SD (n = 3).



**Figure 15. Crosstalk between Sesn1/2/3 and mTORC1, ER stress, and oxidative stress in the regulation of JNK.** (A–C) Immunoblotting and quantification analysis of mTORC1 signaling (p-S6 as a readout) and JNK activation (p-JNK as a readout) in the control and *SESN1/2/3* KD HepG2 cells after 2-hour pretreatment with either vehicle or 20 nmol/L rapamycin, followed by incubation with 200  $\mu$ mol/L PA for 24 hours. (D–F) Immunoblotting and quantification analysis of PERK and JNK activation (p-eIF2 $\alpha$  and p-JNK as a readout, respectively) in the control and *SESN1/2/3* KD HepG2 cells after 2-hour pretreatment with vehicle or 2  $\mu$ mol/L GSK2656157 (a PERK inhibitor), followed by incubation with 200  $\mu$ mol/L PA for 24 hours. (G–I) Immunoblotting and quantification analysis of oxidative stress (MDA modified proteins as a readout) in the control and *SESN1/2/3* KD HepG2 cells after 2-hour pretreatment with vehicle or 5 mmol/L N-acetyl cysteine (NAC), followed by incubation with 200  $\mu$ mol/L PA for 24 hours. Data are expressed as mean  $\pm$  SD (n = 3).



### Protein Analysis

Total protein and phosphorylated protein levels were analyzed by immunoblotting after sodium dodecyl sulfate-gel electrophoresis. The following antibodies were used for the immunoblots: anti-p-NF- $\kappa$ B (Ser536; Cell Signaling Technology, Danvers, MA; #3033), anti-NF- $\kappa$ B (Cell Signaling Technology; #8242), anti-p-JNK (Thr183/Tyr185; Cell Signaling Technology; #4668), anti-JNK (Cell Signaling Technology; #9258), and anti-p-c-Jun (Ser63; Cell Signaling Technology; #9261). Immunoprecipitation was performed in HepG2 or Huh7 cells after transfection of indicated DNA constructs. Immunoprecipitation and immunoblotting were performed using tag antibodies: mouse monoclonal anti-FLAG M2 affinity gel (Sigma-Aldrich; #A2220) and rabbit anti-HA tag antibody (Cell Signaling Technology; #3724).

### Histologic Analysis

Tissue samples were fixed in neutral formalin solution (10%) and then processed for embedding and sectioning at the Histology Core of Indiana University School of Medicine. Liver sections (4- $\mu$ m thickness) were stained with H&E or Sirius Red dye according to the standard protocols. Cell death in liver sections was analyzed using an ApopTag peroxidase in situ apoptosis detection kit (Sigma-Millipore, Burlington, MA) by following the kit manual. To examine hepatic oxidative stress, inflammation, and fibrotic alterations, we performed immunofluorescence analysis of fixed liver sections. After deparaffinization and rehydration, the liver sections were incubated with 2.5% normal horse serum for 1 hour at room temperature and then with the following primary antibodies: mouse anti-4-HNE monoclonal antibody (R&D Systems; MAB3249, 1:250), mouse

**Table 1.** DNA Oligonucleotide Sequences

Gene	Species	Primer sequence (forward and reverse)	Application
<i>Srebp1a</i>	Mouse	5'-GAA CAG ACA CTG GCC GAG AT-3' 5'-AGC TGG AGC ATG TCT TCG AT-3'	qPCR
<i>Srebp1c</i>	Mouse	5'- GGA GCC ATG GAT TGC ACA TT -3'' 5'- CCT GTC TCA CCC CCA GCA TA -3'	qPCR
<i>Fasn</i>	Mouse	5'- CTG CCA CAA CTC TGA GGA CA-3'' 5'- TTC GTA CCT CCT TGG CAA AC -3'	qPCR
<i>Dgat1</i>	Mouse	5'- ACA GAG ACC ACC AGC ACA AC-3'' 5'- ATT CAT CCT GTC TCG GAC TGC -3'	qPCR
<i>Dgat2</i>	Mouse	5'- TTC CTG GCA TAA GGC CCT ATT-3'' 5'- AGT CTA TGG TGT CTC GGT TGA C-3'	qPCR
<i>Fasn</i>	Mouse	5'- CTG CCA CAA CTC TGA GGA CA-3'' 5'- TTC GTA CCT CCT TGG CAA AC -3'	qPCR
<i>Scd</i>	Mouse	5'-GCG TTC CAG AAT GAC GTG TA-3'' 5'-CCA ACC CAC GTG AGA GAA GA-3'	qPCR
<i>Gss</i>	Mouse	5'- TGT GCC CTT TTA CCC TCT TCC T -3'' 5'- TCT TTG GAG TGT GGG AAT GGA -3'	qPCR
<i>Gpx3</i>	Mouse	5'- GCT TGG TCA TTC TGG GCT TC -3' 5'- CCC ACC TGG TCG AAC ATA CT -3'	qPCR
<i>Sod1</i>	Mouse	5'- TTG GCC GTA CAA TGG TGG T-3' 5'- CGC AAT CCC AAT CAC TCC AC -3'	qPCR
<i>Sod2</i>	Mouse	5'- GGT GGC GTT GAG ATT GTT CA -3' 5'- CCC AGA CCT GCC TTA CGA CTAT -3'	qPCR
<i>Sod3</i>	Mouse	5'-CTT GTT CTA CGG CTT GCT GCT ACT G-3' 5'- ATG CGT GTC GCC TAT CTT CT-3'	qPCR
<i>Cat</i>	Mouse	5'- TCA CCC ACG ATA TCA CCA GA -3' 5'- AGC TGA GCC TGA CTC TCC AG -3'	qPCR
<i>Nox1</i>	Mouse	5'- TGG AGT GGC TTG ACC-3' 5'- TGC TGC CAT GAC CAA CCT TTT-3'	qPCR
<i>Nox2</i>	Mouse	5'- TTT ACA CTG ACA TCC GCC CC-3' 5'- TGG GCC GTC CAT ACA AAG TC-3'	qPCR
<i>Mpo</i>	Mouse	5'- GCC AAG GCC TTT CAA TGT TA-3' 5'- TCA CGT CCT GAT AGG CAC AG-3'	qPCR
<i>Tnf</i>	Mouse	5'- GGC CTC CCT CTC ATC AGT TC-3' 5'- CAC TTG GTG GTT TGC TAC GA-3'	qPCR
<i>Il1b</i>	Mouse	5'- TGT GAA ATG CCA CCT TTT GA-3' 5'-GGT CAA AGG TTT GGA AGC AG-3'	qPCR
<i>Il6</i>	Mouse	5'-CAA AGC CAG AGT CCT TCA GAG-3' 5'-GAG CAT TGG AAA TTG GGG TA-3'	qPCR
<i>Il10</i>	Mouse	5'- CAG AGC CAC ATG CTC CTA GA-3' 5'-GCT TGG CAA CCC AAG TAA CC-3'	qPCR
<i>Tgfb1</i>	Mouse	5'-CGC AAC AAC GCC ATC TAT GA 5'-ACT GCT TCC CGA ATG TCT GA	qPCR
<i>Tgfb2</i>	Mouse	5'-CGC AAC AAC GCC ATC TAT GA 5'-ACT GCT TCC CGA ATG TCT GA	qPCR
<i>Pdgfbr</i>	Mouse	5'-CAT TTG CAA AAC CAC CAT TG 5'-GGC ATT CAC AGA GAC GTT GA	qPCR
<i>Mmp2</i>	Mouse	5'-ACT CCG GAG ATC TGC AAA CA 5'-ACT GTC CGC CAA ATA AAC CG	qPCR
<i>Timp1</i>	Mouse	5'-CAT GGA AAG CCT CTG TGG AT 5'-CTC AGA GTA CGC CAG GGA AC	qPCR
<i>Acta2</i>	Mouse	5'-AGG CAC CAC TGA ACC CTA AG 5'-GAC AGC ACA GCC TGA ATA GC	qPCR
<i>Col1a1</i>	Mouse	5'-CAC CTG GTC CAC AAG GTT TC 5'-CCC ATC ATC TCC ATT CTT GC	qPCR
<i>Col4a1</i>	Mouse	5'-TTC GCC TCC AGG AAC GAC TA 5'-AAA CCG CAC ACC TGC TAA TG	qPCR

Table 1. Continued

Gene	Species	Primer sequence (forward and reverse)	Application
<i>Ppia</i>	Mouse	5'-CAC CGT GTT CTT CGA CAT CA-3' 5'-CAG TGC TCA GAG CTC GAA AGT-3'	qPCR
<i>Floxed Sesn1</i>	Mouse	5'-GCATGCCATGTAATACACCAACA-3' 5'-GAAGTGATTGGCAGGATGTGTG-3'	Genotyping
<i>Sesn2 knockout</i>	Mouse	5'-GGTCAGAGGAAGTGCATAGGA-3' 5'-CCAACCCCTCCTCCTACAT-3' 5'-CTCACCAGCCCCTGTTTTTA-3'	Genotyping
<i>Floxed Sesn3</i>	Mouse	5'-GTTGTGCAAACACCATGC-3' 5'-CTACAGGTTTATGTATTTGCTATCTATG-3'	Genotyping
<i>SESN1 sgRNA</i>	Human	5'-ATTCCTCGACCACTAGGACA-3'	CRISPR/Cas9
<i>SESN2 sgRNA</i>	Human	5'-CAGGTTGTCTACTCGCCAG-3'	CRISPR/Cas9
<i>SESN3 sgRNA</i>	Human	5'-AGCTGCTAGCACATCGACCT-3'	CRISPR/Cas9

*Acta2*, smooth muscle actin alpha 2; *Col1a1*, collagen type 1a1; *Col4a1*, collagen type 4a1; *Cpt1a*, carnitine palmitoyl-transferase 1A; *Fasn*, fatty acid synthase; *Gpx*, glutathione peroxidase; *Gsr*, glutathione reductase; *Gss*, glutathione synthetase; *Il1b*, interleukin-1 beta; *Mmp2*, matrix metalloproteinase 2; *Pdgfrb*, platelet-derived growth factor receptor beta; *Ppia*, peptidylprolyl isomerase A; *Sod*, superoxide dismutase; *Srebp1*, sterol regulatory element binding transcription factor 1; *tgfr*, transforming growth factor beta receptor; *tgfb1*, transforming growth factor 1; *Timp1*, tissue inhibitor of metalloproteinase 1; *Tnf*, tumor necrosis factor-alpha.

anti-F4/80 monoclonal antibody (Invitrogen; MA5-16363, 1:250), rabbit anti-MPO polyclonal antibody (Invitrogen; PA5-16672, 1:250), rabbit anti-TIMP-1 polyclonal antibody (Proteintech, Rosemont, IL; #16644-1-AP, 1:200), rabbit anti- $\alpha$ SMA polyclonal antibody (Abcam, Cambridge, MA; ab5694, 1:200), and rabbit anti-phospho-SAPK/JNK (Thr183/Tyr185; Cell Signaling Technology; #4668, 1:200). Next, the following fluorophore-conjugated secondary antibodies were applied to the sections: goat anti-rabbit immunoglobulin G (H+L) Alexa Fluor 488 (Invitrogen; A11034), goat anti-mouse immunoglobulin G (H+L) Alexa Fluor 488 (Invitrogen; A11001), donkey anti-rabbit immunoglobulin G (H+L) Alexa Fluor 594 (Invitrogen; A21207), and goat anti-mouse immunoglobulin G (H+L) Alexa Fluor 594 (Invitrogen; A11032). Images for H&E or Sirius Red staining were captured using a Leica DM750 microscope (Wetzlar, Germany) equipped with EC3 digital camera and LAS EZ software (Buffalo Grove, IL). Immunofluorescence images were obtained by a Zeiss fluorescence microscope (Oberkochen, Germany) using AxioVision Rel 4.8 software (White Plains, NY). Positive signals were quantified from the randomly selected sections at least 5 fields per sample using Image J 1.64 software (NIH, Bethesda, MD).

### Cell Culture and Generation of SESN1/2/3-Deficient Cell Line Using CRISPR-Cas9

Human hepatoma cell line HepG2 cells were cultured in Dulbecco modified Eagle medium supplemented with 10% fetal bovine serum, 100 U/mL penicillin, and 100  $\mu$ g/mL streptomycin (Thermo Fisher Scientific) in an incubator under conditions of 37°C and 5% CO<sub>2</sub>. To generate SESN1/2/3 KD HepG2 cells, we designed single guide RNAs (sgRNAs) targeting human SESN1/2/3 coding sequences using the GPP sgRNA Designer on the Broad Institute website and cloned the sgRNAs into a lentiCRISPR v2 vector

as a gift from Dr Feng Zhang (Addgene, Cambridge, MA; #52961; <http://n2t.net/addgene:52961>; RRID:Addgene\_52961).<sup>45</sup> To induce lipotoxicity, HepG2, Huh7, and mouse primary hepatocytes were treated with 200  $\mu$ mol/L PA (Sigma-Aldrich) or control vehicle BSA. Cells were seeded at  $2.5 \times 10^5$  cells/dish or well (35-mm glass bottom dish or 6-well plates) and then treated with 200  $\mu$ mol/L PA for 18 hours. After incubation, cells were washed and rinsed for further analysis by immunocytochemistry or immunoblotting. For immunocytochemistry, cells were incubated with 2.5% normal horse serum for 40 minutes and then with primary antibodies. After incubation at 4°C overnight, cells were washed 2 times with phosphate-buffered saline-Tween for 10 minutes each and 1 time with phosphate-buffered saline for 15 minutes, followed by staining using an ABC-peroxidase kit (Vector Laboratories Inc, Burlingame, CA). To examine the role of JNK in the PA-induced lipotoxicity, cells were pretreated with dimethyl sulfoxide (DMSO) or a JNK inhibitor SP600125 (10  $\mu$ mol/L) for 6 hours before the PA treatment in some experiments. To assess the impact of mTORC1, PERK, and oxidative stress on JNK phosphorylation, WT and SESN1/2/3 KD HepG2 cells were pretreated with rapamycin (20 nmol/L), GSK2656157 (2  $\mu$ mol/L), and N-acetyl cysteine (5 mmol/L) for 2 hours before incubation with 200  $\mu$ mol/L PA for 24 hours.

### Gene Expression Omnibus Data and Statistical Analysis

Human NASH liver microarray data were downloaded from Gene Expression Omnibus (Accession #GSE48452), and SESN1/2/3 gene expression was analyzed.<sup>46</sup> Statistical analysis was performed using Welch's unpaired two-tailed *t* test between 2 groups and one-way or two-way analysis of variance followed by Tukey post hoc tests for multiple groups (GraphPad Prism 9.1.0; San Diego, CA).

## References

1. Bae SH, Sung SH, Oh SY, Lim JM, Lee SK, Park YN, Lee HE, Kang D, Rhee SG. Sestrins activate Nrf2 by promoting p62-dependent autophagic degradation of Keap1 and prevent oxidative liver damage. *Cell Metab* 2013;17:73–84.
2. Budanov AV, Karin M. p53 target genes sestrin1 and sestrin2 connect genotoxic stress and mTOR signaling. *Cell* 2008;134:451–460.
3. Dong XC. The potential of sestrins as therapeutic targets for diabetes. *Expert Opin Ther Targets* 2015;19:1011–1015.
4. Huang M, Kim HG, Zhong X, Dong C, Zhang B, Fang Z, Zhang Y, Lu X, Saxena R, Liu Y, Zhang C, Liangpunsakul S, Dong XC. Sestrin 3 protects against diet-induced nonalcoholic steatohepatitis in mice through suppression of transforming growth factor beta signal transduction. *Hepatology* 2020;71:76–92.
5. Hwang HJ, Jung TW, Choi JH, Lee HJ, Chung HS, Seo JA, Kim SG, Kim NH, Choi KM, Choi DS, Baik SH, Yoo HJ. Knockdown of sestrin2 increases pro-inflammatory reactions and ER stress in the endothelium via an AMPK dependent mechanism. *Biochim Biophys Acta Mol Basis Dis* 2017;1863:1436–1444.
6. Hwang HJ, Kim JW, Chung HS, Seo JA, Kim SG, Kim NH, Choi KM, Baik SH, Yoo HJ. Knockdown of sestrin2 increases lipopolysaccharide-induced oxidative stress, apoptosis, and fibrotic reactions in H9c2 cells and heart tissues of mice via an AMPK-dependent mechanism. *Mediators Inflamm* 2018;2018:6209140.
7. Jegal KH, Park SM, Cho SS, Byun SH, Ku SK, Kim SC, Ki SH, Cho IJ. Activating transcription factor 6-dependent sestrin 2 induction ameliorates ER stress-mediated liver injury. *Biochim Biophys Acta Mol Cell Res* 2017;1864:1295–1307.
8. Kang X, Petyaykina K, Tao R, Xiong X, Dong XC, Liangpunsakul S. The inhibitory effect of ethanol on Sestrin3 in the pathogenesis of ethanol-induced liver injury. *Am J Physiol Gastrointest Liver Physiol* 2014;307:G58–G65.
9. Kim HJ, Joe Y, Kim SK, Park SU, Park J, Chen Y, Kim J, Ryu J, Cho GJ, Surh YJ, Ryter SW, Kim UH, Chung HT. Carbon monoxide protects against hepatic steatosis in mice by inducing sestrin-2 via the PERK-eIF2alpha-ATF4 pathway. *Free Radic Biol Med* 2017;110:81–91.
10. Kim JS, Ro SH, Kim M, Park HW, Semple IA, Park H, Cho US, Wang W, Guan KL, Karin M, Lee JH. Sestrin2 inhibits mTORC1 through modulation of GATOR complexes. *Scientific Reports* 2015;5:9502.
11. Lee JH, Budanov AV, Park EJ, Birse R, Kim TE, Perkins GA, Ocorr K, Ellisman MH, Bodmer R, Bier E, Karin M. Sestrin as a feedback inhibitor of TOR that prevents age-related pathologies. *Science* 2010;327:1223–1228.
12. Lee JH, Budanov AV, Talukdar S, Park EJ, Park HL, Park HW, Bandyopadhyay G, Li N, Aghajan M, Jang I, Wolfe AM, Perkins GA, Ellisman MH, Bier E, Scadeng M, Foretz M, Viollet B, Olefsky J, Karin M. Maintenance of metabolic homeostasis by Sestrin2 and Sestrin3. *Cell Metab* 2012;16:311–321.
13. Liu Y, Kim HG, Dong E, Dong C, Huang M, Liu Y, Liangpunsakul S, Dong XC. Sestrin3 deficiency promotes carcinogen-induced hepatocellular carcinoma via regulation of the hedgehog pathway. *Biochim Biophys Acta Mol Basis Dis* 2019;1865:2685–2693.
14. Park HW, Park H, Ro SH, Jang I, Semple IA, Kim DN, Kim M, Nam M, Zhang D, Yin L, Lee JH. Hepatoprotective role of Sestrin2 against chronic ER stress. *Nat Commun* 2014;5:4233.
15. Ro SH, Nam M, Jang I, Park HW, Park H, Semple IA, Kim M, Kim JS, Park H, Einat P, Damari G, Golikov M, Feinstein E, Lee JH. Sestrin2 inhibits uncoupling protein 1 expression through suppressing reactive oxygen species. *Proc Natl Acad Sci U S A* 2014;111:7849–7854.
16. Tao R, Xiong X, Liangpunsakul S, Dong XC. Sestrin 3 protein enhances hepatic insulin sensitivity by direct activation of the mTORC2-Akt signaling. *Diabetes* 2015;64:1211–1223.
17. Kim H, An S, Ro SH, Teixeira F, Jin Park G, Kim C, Cho CS, Kim JS, Jakob U, Hee Lee J, Cho US. Janus-faced Sestrin2 controls ROS and mTOR signalling through two separate functional domains. *Nat Commun* 2015;6:10025.
18. Chantranupong L, Wolfson RL, Orozco JM, Saxton RA, Scaria SM, Bar-Peled L, Spooner E, Isasa M, Gygi SP, Sabatini DM. The Sestrins interact with GATOR2 to negatively regulate the amino-acid-sensing pathway upstream of mTORC1. *Cell Reports* 2014;9:1–8.
19. Parmigiani A, Nourbakhsh A, Ding B, Wang W, Kim YC, Akopiants K, Guan KL, Karin M, Budanov AV. Sestrins inhibit mTORC1 kinase activation through the GATOR complex. *Cell Reports* 2014;9:1281–1291.
20. Kowalsky AH, Namkoong S, Mettetal E, Park HW, Kazyken D, Fingar DC, Lee JH. The GATOR2-mTORC2 axis mediates Sestrin2-induced AKT Ser/Thr kinase activation. *J Biol Chem* 2020;295:1769–1780.
21. Velasco-Miguel S, Buckbinder L, Jean P, Gelbert L, Talbott R, Laidlaw J, Seizinger B, Kley N. PA26, a novel target of the p53 tumor suppressor and member of the GADD family of DNA damage and growth arrest inducible genes. *Oncogene* 1999;18:127–137.
22. Garaeva AA, Kovaleva IE, Chumakov PM, Evstafieva AG. Mitochondrial dysfunction induces SESN2 gene expression through activating transcription factor 4. *Cell Cycle* 2016;15:64–71.
23. Byun JK, Choi YK, Kim JH, Jeong JY, Jeon HJ, Kim MK, Hwang I, Lee SY, Lee YM, Lee IK, Park KG. A positive feedback loop between Sestrin2 and mTORC2 is required for the survival of glutamine-depleted lung cancer cells. *Cell Reports* 2017;20:586–599.
24. Zhang XY, Wu XQ, Deng R, Sun T, Feng GK, Zhu XF. Upregulation of sestrin 2 expression via JNK pathway activation contributes to autophagy induction in cancer cells. *Cell Signal* 2013;25:150–158.
25. Chen YS, Chen SD, Wu CL, Huang SS, Yang DI. Induction of sestrin2 as an endogenous protective mechanism against amyloid beta-peptide neurotoxicity in primary cortical culture. *Exp Neurol* 2014;253:63–71.



26. Shin BY, Jin SH, Cho IJ, Ki SH. Nrf2-ARE pathway regulates induction of Sestrin-2 expression. *Free Radic Biol Med* 2012;53:834–841.
27. Shi X, Doycheva DM, Xu L, Tang J, Yan M, Zhang JH. Sestrin2 induced by hypoxia inducible factor1 alpha protects the blood-brain barrier via inhibiting VEGF after severe hypoxic-ischemic injury in neonatal rats. *Neurobiol Dis* 2016;95:111–121.
28. Budanov AV, Shoshani T, Faerman A, Zelin E, Kamer I, Kalinski H, Gorodin S, Fishman A, Chajut A, Einat P, Skaliter R, Gudkov AV, Chumakov PM, Feinstein E. Identification of a novel stress-responsive gene Hi95 involved in regulation of cell viability. *Oncogene* 2002;21:6017–6031.
29. Ding B, Parmigiani A, Divakaruni AS, Archer K, Murphy AN, Budanov AV. Sestrin2 is induced by glucose starvation via the unfolded protein response and protects cells from non-canonical necroptotic cell death. *Scientific Reports* 2016;6:22538.
30. Chen CC, Jeon SM, Bhaskar PT, Nogueira V, Sundararajan D, Tonic I, Park Y, Hay N. FoxOs inhibit mTORC1 and activate Akt by inducing the expression of Sestrin3 and Rictor. *Dev Cell* 2010;18:592–604.
31. Hagenbuchner J, Kuznetsov A, Hermann M, Hausott B, Obexer P, Ausserlechner MJ. FOXO3-induced reactive oxygen species are regulated by BCL2L1 (Bim) and SESN3. *J Cell Sci* 2012;125(Pt 5):1191–1203.
32. Peng M, Yin N, Li MO. Sestrins function as guanine nucleotide dissociation inhibitors for Rag GTPases to control mTORC1 signaling. *Cell* 2014;159:122–133.
33. Kim M, Sujkowski A, Namkoong S, Gu B, Cobb T, Kim B, Kowalsky AH, Cho CS, Semple I, Ro SH, Davis C, Brooks SV, Karin M, Wessells RJ, Lee JH. Sestrins are evolutionarily conserved mediators of exercise benefits. *Nat Commun* 2020;11:190.
34. Segales J, Perdiguero E, Serrano AL, Sousa-Victor P, Ortet L, Jardi M, Budanov AV, Garcia-Prat L, Sandri M, Thomson DM, Karin M, Hee Lee J, Munoz-Canoves P. Sestrin prevents atrophy of disused and aging muscles by integrating anabolic and catabolic signals. *Nat Commun* 2020;11:189.
35. Ebnoether E, Ramseier A, Cortada M, Bodmer D, Levano-Huaman S. Sesn2 gene ablation enhances susceptibility to gentamicin-induced hair cell death via modulation of AMPK/mTOR signaling. *Cell Death Discov* 2017;3:17024.
36. Li R, Huang Y, Semple I, Kim M, Zhang Z, Lee JH. Cardioprotective roles of sestrin 1 and sestrin 2 against doxorubicin cardiotoxicity. *Am J Physiol Heart Circ Physiol* 2019;317:H39–H48.
37. Svegliati-Baroni G, Pierantonelli I, Torquato P, Marinelli R, Ferreri C, Chatgililoglu C, Bartolini D, Galli F. Lipidomic biomarkers and mechanisms of lipotoxicity in non-alcoholic fatty liver disease. *Free Radic Biol Med* 2019;144:293–309.
38. Yang JH, Kim KM, Cho SS, Shin SM, Ka SO, Na CS, Park BH, Jegal KH, Kim JK, Ku SK, Lee HJ, Park SG, Cho IJ, Ki SH. Inhibitory effect of Sestrin 2 on hepatic stellate cell activation and liver fibrosis. *Antioxid Redox Signal* 2019;31:243–259.
39. Hu YB, Ye XT, Zhou QQ, Fu RQ. Sestrin 2 attenuates rat hepatic stellate cell (HSC) activation and liver fibrosis via an mTOR/AMPK-dependent mechanism. *Cell Physiol Biochem* 2018;51:2111–2122.
40. Kim SJ, Kim KM, Yang JH, Cho SS, Kim JY, Park SJ, Lee SK, Ku SK, Cho IJ, Ki SH. Sestrin2 protects against acetaminophen-induced liver injury. *Chem Biol Interact* 2017;269:50–58.
41. Jin SH, Yang JH, Shin BY, Seo K, Shin SM, Cho IJ, Ki SH. Resveratrol inhibits LXRA $\alpha$ -dependent hepatic lipogenesis through novel antioxidant Sestrin2 gene induction. *Toxicol Appl Pharmacol* 2013;271:95–105.
42. Win S, Than TA, Zhang J, Oo C, Min RWM, Kaplowitz N. New insights into the role and mechanism of c-Jun-N-terminal kinase signaling in the pathobiology of liver diseases. *Hepatology* 2018;67:2013–2024.
43. Lanna A, Gomes DC, Muller-Durovic B, McDonnell T, Escors D, Gilroy DW, Lee JH, Karin M, Akbar AN. A sestrin-dependent Erk-Jnk-p38 MAPK activation complex inhibits immunity during aging. *Nat Immunol* 2017;18:354–363.
44. Park JG, Aziz N, Cho JY. MKK7, the essential regulator of JNK signaling involved in cancer cell survival: a newly emerging anticancer therapeutic target. *Ther Adv Med Oncol* 2019;11:1758835919875574.
45. Sanjana NE, Shalem O, Zhang F. Improved vectors and genome-wide libraries for CRISPR screening. *Nature Methods* 2014;11:783–784.
46. Ahrens M, Ammerpohl O, von Schonfels W, Kolarova J, Bens S, Itzel T, Teufel A, Herrmann A, Brosch M, Hinrichsen H, Erhart W, Egberts J, Sipos B, Schreiber S, Hasler R, Stickel F, Becker T, Krawczak M, Rocken C, Siebert R, Schafmayer C, Hampe J. DNA methylation analysis in nonalcoholic fatty liver disease suggests distinct disease-specific and remodeling signatures after bariatric surgery. *Cell Metab* 2013;18:296–302.

---

Received September 7, 2020. Accepted April 26, 2021.

#### Correspondence

Address correspondence to: X. Charlie Dong, PhD, Department of Biochemistry and Molecular Biology, Indiana University School of Medicine, 635 Barnhill Drive, MS 1021D, Indianapolis, Indiana 46202. e-mail: xcdong@iu.edu; fax: (317) 274-4686.

#### Acknowledgments

The authors thank Dr Guoli Dai for providing the Huh7 cells, Dr Lindsey Mayo for providing the JNK inhibitors, and Drs Ronald Wek and Kirk Staschke for providing the PERK inhibitor.

All authors had access to the study data, reviewed, and approved the final manuscript.

#### CRedit Authorship Contributions

Zhigang Fang (Investigation: Lead; Methodology: Lead; Writing – original draft: Supporting)

Hyeong-Geug Kim (Investigation: Lead; Methodology: Lead; Writing – original draft: Supporting)

Menghao Huang (Investigation: Supporting; Methodology: Supporting; Writing – original draft: Supporting)

Kushan Chowdhury (Investigation: Supporting; Methodology: Supporting; Writing – review & editing: Supporting)

Ming O. Li (Resources: Supporting)

Suthat Liangpunsakul (Funding acquisition: Equal; Supervision: Supporting; Writing – original draft: Supporting)

X. Charlie Dong, PhD (Conceptualization: Lead; Data curation: Lead; Formal analysis: Lead; Funding acquisition: Equal; Investigation: Supporting; Methodology: Supporting; Project administration: Lead; Supervision: Lead; Writing – original draft: Lead; Writing – review & editing: Lead)

**Conflicts of interest**

The authors disclose no conflicts.

**Funding**

Supported in part by the following funding sources: US National Institutes of Health (NIH) R01DK120689 (X. Charlie Dong), R01DK121925 (X. Charlie Dong), R56DK091592 (X. Charlie Dong), R21AA024550 (X. Charlie Dong), R01DK107682 (Suthat Liangpunsakul and X. Charlie Dong), Indiana Clinical and Translational Sciences Institute funded by the NIH NCATS CTSA UL1TR002529, and a visiting research scholarship from Guangzhou University of Chinese Medicine (Zhigang Fang). The sponsors had no role in the study design and data collection, analysis, and interpretation.